# LTE in unlicensed spectrum: indoor planning, performance evaluation, and coexistence with WiFi

Omar Sandoval Mendoza

**School of Electrical Engineering**

Thesis submitted for examination for the degree of Master of Science in Technology.

Espoo 22.5.2016

**Thesis supervisor:**

Prof. Jyri Hämäläinen

**Thesis advisor:**

Ph.D. David González G.

Aalto University
School of Electrical
Engineering

AALTO UNIVERSITY
SCHOOL OF ELECTRICAL ENGINEERING

ABSTRACT OF THE
MASTER'S THESIS

Author: Omar Sandoval Mendoza

Title: LTE in unlicensed spectrum: indoor planning, performance evaluation, and coexistence with WiFi

Date: 22.5.2016 Language: English Number of pages: 8+61

Department of Communications and Networking

Professorship: Advanced Radio Systems

Supervisor: Prof. Jyri Hämäläinen

Advisor: Ph.D. David González G.

The pursuit of more bandwidth and more efficient spectrum usage has led to consider the use of Long Term Evolution (LTE) technology in unlicensed spectrum, a concept particularly useful for indoor deployments. However, LTE must be modified in order to guarantee a fair coexistence with other systems, particularly WiFi.

There exist several coexistence methods, such as listen-before-talk (LBT), advanced channel selection, duty cycle, and variations of them. Research into unlicensed spectrum has focused into LTE Licensed Assisted Access (LAA) and LTE-Unlicensed (LTE-U), expected to be specified in 2016.

The contribution of this thesis is complementary to the current work, and is focused on coexistence from the perspective of network planning and radio access optimization. This is accomplished with a framework that yields optimized network topologies that maximize the benefits from the LTE deployment, fulfill coverage criteria, and minimize interference. The efficacy of the statistically optimized network topologies has also been validated by means of system level simulations.

Keywords: 5G, indoor planning, multiobjective optimization, LTE

# Preface

I want to thank Professor Jyri Hämäläinen for giving me the opportunity to work on this thesis, and to M.Sc. Saray Renilla for her guidance during the initial stages of research.

I am particularly grateful to my advisor Ph.D. David González G. for his continuous support and guidance through all the changes that this thesis had. This thesis would not be possible without his insightful comments and encouragement.

Last but not least, I would like to thank my parents, and my brother for their love and support during my studies.

Otaniemi, 22.5.2016

Omar Sandoval Mendoza

# Contents

**Abstract** **ii**

**Preface** **iii**

**Contents** **iv**

**Symbols and abbreviations** **vi**

**1 Introduction** **1**
1.1 Context & Motivation . . . . . 1
1.2 Contribution . . . . . 3
1.3 Thesis Outline . . . . . 4

**2 LTE in Unlicensed Spectrum** **5**
2.1 Introduction to LTE . . . . . 5
2.2 LTE Frame Structure . . . . . 6
2.3 LTE Multiple Access . . . . . 8
2.3.1 Downlink: OFDMA . . . . . 8
2.3.2 Uplink: SC-FDMA . . . . . 10
2.4 LTE-Advanced . . . . . 11
2.4.1 Carrier Aggregation . . . . . 12
2.5 Virtualization techniques . . . . . 14
2.6 LTE in unlicensed spectrum . . . . . 15
2.6.1 Regulations in the 5 GHz band . . . . . 16
2.6.2 Coexistence with WiFi . . . . . 17
2.6.3 Current research . . . . . 19
2.7 Remarks . . . . . 24

**3 Proposed Framework** **26**
3.1 Indoor environment and channel characterization . . . . . 27
3.1.1 Indoor channel characterization . . . . . 28
3.2 Multiobjective optimization and NSGA-II . . . . . 32
3.3 System-level simulations . . . . . 35
3.3.1 Link-level and system-level simulations . . . . . 36
3.3.2 Structure and overview of the simulator . . . . . 36
3.4 Remarks . . . . . 38

**4 System Model and Network Optimization** **40**
4.1 System model . . . . . 40
4.2 Indoor planing optimization . . . . . 44
4.2.1 Multiobjective optimization formulation . . . . . 44
4.3 Remarks . . . . . 45

**5 Performance Evaluation** **47**
5.1 Test case & parameter settings . . . . . 47
5.2 Multiobjective evolutionary optimization . . . . . 48
5.3 System-Level Simulations . . . . . 50
5.4 Remarks . . . . . 53

**6 Conclusions and Future Work** **54**
6.1 Conclusions . . . . . 54
6.2 Future work . . . . . 55

**References** **56**

# Symbols and abbreviations

## Symbols

| | |
|---|---|
| $\alpha$ | Average load |
| $\delta_{\mathrm{L}}$ | Service spatial distribution |
| $\gamma$ | SINR |
| $\boldsymbol{\eta}$ | Spectral efficiency |
| $\rho$ | Traffic asymmetry |
| $\mathcal{A}$ | Coverage area |
| $a$ | Area element |
| $B_{ch}$ | System bandwidth |
| $\mathbf{I}$ | Interference |
| $l$ | LTE-U Node |
| $L_{\mathrm{W}}$ | Number of WiFi APs |
| $L_{\mathrm{L}}$ | Number of LTE-U candidate locations |
| $G$ | Antennas gain matrix |
| $\mathbf{P}$ | Received power |
| $P^{\mathrm{CAA+}}$ | Clear channel assessment probability |
| $P^{\mathrm{tx}}$ | Transmission power |
| $R_{TH}$ | Target rate |
| $\mathbf{S}$ | Coverage matrix |
| $\mathbf{x}$ | Topology vector |
| $z_i$ | Bernoulli random variable |

## Operators

| | |
|---|---|
| $\odot$ | Pointwise multiplication |
| $\oslash$ | Pointwise division |
| $\sum_i$ | Sum over index $i$ |
| $\mathbf{A} \cdot \mathbf{B}$ | dot product of vectors $\mathbf{A}$ and $\mathbf{B}$ |

## Abbreviations

| | |
|---|---|
| 3G | 3rd Generation |
| 3GPP | 3rd Generation Partnership Project |
| 4G | 4th Generation |
| 5G | 5th Generation |
| AP | Access Point |
| BBU | Base Band Unit |
| BLER | Block Error Rate |
| C-RAN | Cloud-Radio Access Network |
| CA | Carrier Aggregation |
| CA | Collision Avoidance |
| CC | Component Carrier |
| CCA | Clear Channel Assessment |
| CDF | Cumulative Distribution Function |
| CDMA | Code Division Multiple Access |
| CSAT | Carrier-Sensing Adaptive Transmission |
| CSMA | Carrier Sense Multiple Access |
| CSI | Channel-State Informatin |
| CSO | Cell Switch Off |
| CP | Cyclic Prefix |
| CQI | Channel Quality Indicator |
| DC | Duty Cycle |
| DL | Downlink |
| DCF | Distributed Coordinated Function |
| DCS | Dynamic Channel Selection |
| DFS | Dynamic Frequency Selection |
| EIRP | Equivalent Isotropically Radiated Power |
| ETSI | European Telecommunications Standards Institute |
| FCC | Federal Communications Commission |
| FDTD | Finite Difference Time Domain |
| FDD | Frequency Division Duplexing |
| FDM | Frequency Division Multiplexing |
| FTP | File Transfer Protocol |
| GA | Genetic Algorithm |
| GRMS | Gaussian Root Mean Square |
| IEEE | Institute of Electrical and Electronics Engineers |
| ISI | Inter-Symbol Interference |
| ISM | Industrial, Scientific, and Medic |
| ITU | International Telecommunication Union |
| ITU-R | International Telecommunication Union-Radiocommunication sector |
| HSDPA | High-Speed Downlink Packet Access |
| L2S | Link-to-System |
| LAA | Licensed Assisted Access |
| LBT | Listen-Before-Talk |
| LDS | LTE-U Discovery Signals |

| | |
|---|---|
| LTE | Long Term Evolution |
| LTE-A | Long Term Evolution Advanced |
| LTE-U | Long Term Evolution Unlicensed |
| MO | Multiobjective Optimization |
| MOEA | Multiobjective Evolutionary Algorithm |
| NFV | Network Function Virtualization |
| NSGA-II | Nondominated Sorting Genetic Algorithm II |
| OFDM | Orthogonal Frequency Division Multiplexing |
| OFDMA | Orthogonal Frequency Division Multiple Access |
| PAPR | Peak-to-Average Power Ratio |
| PC | Power Control |
| PCC | Primary Component Carrier |
| PS | Pilot Symbol |
| QAM | Quadrature Amplitude Modulation |
| QoS | Quality-of-Service |
| QPSK | Quadrature Phase-Shift Key |
| RRU | Radio Resource Unit |
| RLAN | Radio Local Area Network |
| RAN | Radio Access Network |
| RAT | Radio Access Technology |
| RB | Resource Block |
| Rel | Release |
| RLAN | Radio Local Access Network |
| RRM | Radio Resource Management |
| RT | Ray Tracing |
| SCC | Secondary Component Carrier |
| SC-FDMA | Single Carrier Frequency Division Multiple Access |
| SDL | Supplemental Downlink |
| SDN | Software Defined Network |
| SLS | System-Level Simulations |
| SNR | Signal-to-Noise Ratio |
| SINR | Signal-to-Interference-plus-Noise Ratio |
| TDD | Time Division Duplexing |
| TTI | Transmission Time Interval |
| UE | User Equipment |
| UDN | Ultra Dense Networks |
| UL | Uplink |
| U-NII | Unlicensed National Information Infrastructure |
| WAS | Wireless Access Systems |

# 1 Introduction

## 1.1 Context & Motivation

During the last decade, mobile communications have experienced a continuous growth driven by the increasing amount of subscriptions, greater coverage area and users' demand for higher data rates. The Ericsson Mobility Report [1] from June 2014 estimates that the mobile data traffic between 2013 and 2019 will increase tenfold, and by 2021 there will be a total of 9.1 billion mobile subscriptions.

Due to technological improvements, mobile data traffic will increase from 5.3 EB/month in 2015 to 51 EB/month by 2021 [1], representing an annual growth data traffic of 45%. From this forecast, mobile video content will generate most of mobile data traffic. According to [1], [2], mobile video already represents around 50% of total service demand and it will account for as much as 70% of total data traffic by 2021.

It is specially important to point out that up to 80 % of mobile data traffic is generated indoors [3], where coverage is provided by either indoor solutions, or outdoor solutions, or both. Indoor scenarios are more challenging than outdoor since buildings present high attenuation of radio signals, and hence, guaranteeing good coverage is often difficult. Nevertheless, effective indoor solutions are crucial to operators, in order to provide indoor users the same Quality-of-Service (QoS) experienced by outdoor users.

As users continue consuming increasing amounts of data in mobile applications in the following years, mobile networks have to find new solutions to meet the users' demand. Currently, there are several dominant paradigms to boost the capacity of cellular networks, such as allocating more spectrum; densify the network with small cells overlaid on macrocells; increase the network efficiency with multiple antenna techniques, higher order modulation schemes, better coding schemes, among others.

Ultra Dense Networks (UDN), i.e., a very high number of small cells in the same area, call for interference management methods, since the the frequency reuse is very high. In dense deployments of small cells, interference management may become complex and spectrum may easily be congested [4]. Nevertheless, despite these technical challenges, increasing the amount of spectrum to mobile networks has been identified as a clear solution to rapidly increase capacity.

Projections by [5] estimate that larger spectrum is needed to satisfy the growing traffic demand in US, with a deficit of 66 MHz as soon as in 2018. In consequence, it is critical to allocate more spectrum for the current and future mobile communications. However, finding available spectrum and allocating it to mobile networks is not a trivial matter, since spectrum is a finite and expensive resource. In addition, the spectrum between 0 and 6 GHz has appropriate propagation characteristics for mobile communications [6].

The ITU Radiocommunication Sector (ITU-R) is the organization that coordinates the international spectrum usage in the world and decides along with countries the licensed frequency bands that are best suited for radio access technologies [7]. ITU-R holds the World Radiocommunication Conference (WRC) for this purpose every

three to four years, and then emits a series of recommendations and regulations for all the different world regions. Spectrum allocation is done in a per country basis, and the release and bidding of new spectrum can take years, especially if the recommended bands are being used by existing radio technologies. Thus, the contrast between necessary high data rates in the near future and the time and cost of allocating new free spectrum made the industry to look for other frequency bands, mainly millimeter-waves and unlicensed spectrum.

Unlicensed spectrum is free for anyone to use as long as the system complies with the band regulations. The best known unlicensed band, the 2.4 GHz ISM band is already crowded with many devices and Radio Access Technologies (RATs) such as IEEE 802.11 (Wi-Fi) and IEEE 802.15 (Bluetooth). On the other side, the 5 GHz band has many aspects that make it attractive for mobile communications. It has relatively good channel propagation [7], and it also has wide spectrum available even if it is already utilized by Wi-Fi and other RATs. In many cases, there are at least 200 MHz up to 525 MHz according to Figure 1 shows the available unlicensed spectrum in some regions in the world according to [8].

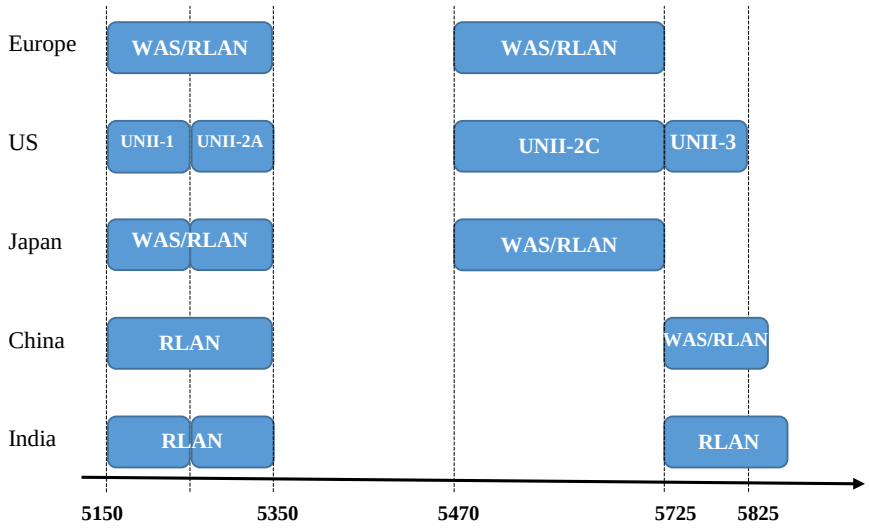


Figure 1: Available spectrum in the 5 GHz band.

Mobile networks operating in unlicensed spectrum and in higher frequencies as millimeter-wave (> 30 GHz) are being intensively investigated for the 5$^{th}$ generation (5G) of mobile networks, expected to be commercialized as early as 2020. 5G research and development is aimed to be an ecosystem that will support many different kinds of use cases, and will do so by fulfilling three different broad targets: a significant increase in capacity, reduced latency, and massive machine type communications [9]. The use of unlicensed spectrum in frequencies below 6 GHz and millimeter-waves above 30 GHz do not conflict each other, rather they are complementary as their propagation characteristics are different. While lower frequencies have propagation

characteristics best suited for outdoor and indoor coverage, higher frequencies can support higher capacity due to the large available spectrum in millimeter-waves.

Thus, bearing in mind the previous context, this thesis will focus on the current research trend of using the 5 GHz unlicensed spectrum to improve LTE capacity. Since LTE was developed as a stand-alone network (i.e., not sharing spectrum), one of the main concerns is LTE fair coexistence with other communication systems. The impact of LTE operating at its current state in unlicensed spectrum has been thoroughly researched in the recent years [10]–[12]. It has been shown that LTE will dominate the spectrum available and will not coexist fairly with other systems. Therefore, one of the main design goals of LTE in unlicensed spectrum is fair coexistence of LTE with other systems, and to follow all regulatory requirements in the 5 GHz band [13].

LTE in unlicensed spectrum research began as early as 2013 [10], [12]. At the moment, two main branches exist: LTE License-Assisted Access (LAA), developed by the 3GPP; and LTE-Unlicensed (LTE-U), developed by the LTE-U Forum, a consortium of private companies including Ericsson, Samsung, Qualcomm and Verizon. Both lines of research rely on the principle of carrier aggregation (CA), introduced in LTE Release 10. This technology allows to increase the overall bandwidth up to 100 MHz, and therefore increase the capacity.

3GPP standards and specifications for LTE LAA are expected to be included in Release 13 in 2016. Initially LAA will be deployed as supplementary downlink (SDL), and it will follow the specification of ETSI for unlicensed spectrum. The main regulations are a limited transmit power and a policy known as Listen Before Talk (LBT) and a maximum transmit power of 40 dBm or 1 Watt. LBT is a mechanism to ensure a good neighbor policy in unlicensed spectrum. A system using LBT, as it name implies, listens to the medium for an amount of time and will transmit only if the received average power is below a threshold. As an example, WiFi uses LBT as a way to confirm the medium is idle, thus avoiding collisions. On the other side, LTE-U Forum was formed in 2014 by Verizon, Alcatel-Lucent, Ericsson, Qualcomm and Samsung. It is a private group effort to develop LTE in unlicensed spectrum in order to market it in the shortest amount of time, and is being developed to work in both UL and DL. Unlike 3GPP, LTE-U does not rely on media sensing, instead it will use a duty cycle based on the amount of networks present to determine media access. The omission of LBT in LTE-U means that it will only be available in markets where LBT is not a coexistence requirement, such as in the US.

## 1.2 Contribution

Taking in consideration the context, and the previous and current work, the direct contribution of this thesis is to present a statistical framework for LTE-U **radio access planning and optimization**. The proposed methodology allows efficient evaluation of LTE-U network topologies and fair coexistence (based on LBT) with existing WiFi deployments. The output of the framework will consist in a set of optimized topologies that can be used as reference for new deployments or for topology adaptation in conjunction with a centralized control.

The proposed framework is shown in Figure 2. The framework involves propaga-

tion characterization using Ray Tracing (RT) techniques; 3D modeling to represent the indoor environment; statistical methods for interference characterization; optimization, and further evaluation of optimized topologies by means of system level simulations. A complete description of the framework is found in Chapter 3 and Chapter 4.

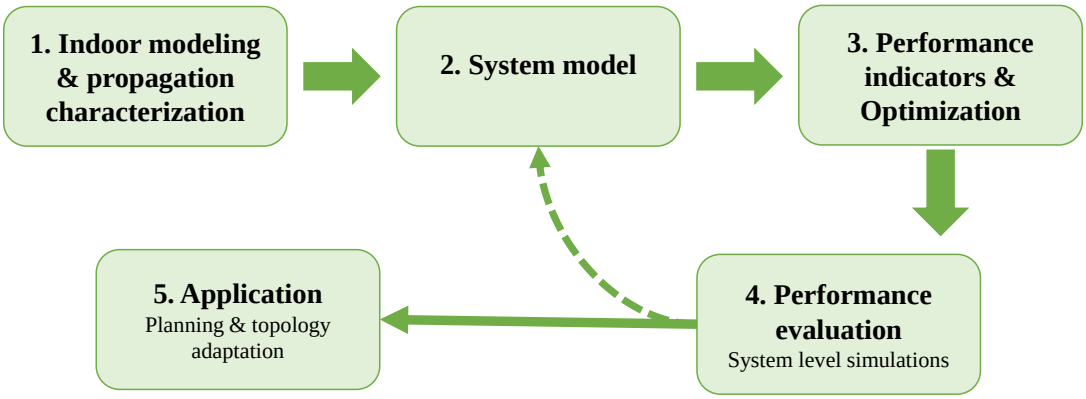


Figure 2: Proposed framework.

## 1.3 Thesis Outline

The thesis is organized as follows:

- **Chapter 2**: introduces relevant aspects of different technologies involved in LTE for unlicensed spectrum, i.e., LTE and Wi-Fi. Additionally, an overview of current LTE in unlicensed spectrum is presented.
- **Chapter 3**: describes in detail the proposed framework.
- **Chapter 4**: describes the system model and optimization problem formulation.
- **Chapter 5**: presents the analysis of numerical results.
- **Chapter 6**: summarizes the conclusions obtained during the document and future research trends.

# 2 LTE in Unlicensed Spectrum

This Chapter reviews the relevant technologies and their characteristics for the development and deployment of LTE in unlicensed spectrum. Firstly, an overview of LTE and LTE-A is presented from section 2.1 to section 2.5, including recent virtualization techniques. Secondly, requirements and state of art of LTE in unlicensed spectrum is summarized in section 2.6.

The scope of this thesis is limited to LTE FDD on the physical layer, and only downlink is considered.

## 2.1 Introduction to LTE

As explained in Chapter 1, the amount of mobile subscribers and data usage of mobile networks has increased constantly since the beginning of the new century. The introduction of third generation 3GPP technologies, such as WCDMA and later HSDPA, helped greatly to increase the offered data rate to match the users' data demand. As an example to portray the rise of mobile data usage, we can see the example of Finland. HSDPA was first introduced in Finland in 2007 and by 2009, data connections carried already ten times more data than voice [14].

Nevertheless, even before the introduction of HSDPA, the increasing traffic demand was already known and it became clear that work on the new radio system should begin [14]. Taking this into account, 3GPP identified the main aspects for the next generation should have [15], and they can be summarized as follows:

- Higher user data rates.
- Improved system capacity and coverage, and reduced overall cost for the operator.
- Potential network and traffic cost reduction.
- Flexible accommodation and deployment of existing and new access technologies with mobility by a common IP-based network.
- Reduced latency.

In November 2004, 3GPP started working on the new mobile generation started during the RAN Evolution Work Shop. A month later, 3GPP started a feasibility study on the evolution of UTRA & UTRAN Long Term Evolution [16]. The performance targets for peak data rate, user throughput and spectrum efficiency were defined relatively to HSPA in Release 6 [15].

Peak data rate:

– Instantaneous downlink peak data rate of 100 Mbps within a 20 MHz downlink spectrum allocation (5 bps/Hz).

– Instantaneous uplink peak data rate of 500 Mbps (2.5 bps/Hz) within a 20 MHz uplink spectrum allocation).

– Transition time of less than 100 ms from a camped state, such as Release 6 Idle Mode, to an active state such as Release 6.

– Transition time of less than 100 ms between a dormant state such as Release 6 and an active state such as Release 6.

User throughput:

– Downlink: average user throughput per MHz, 3 to 4 times Release 6 HSDPA.

– Uplink: average user throughput per MHz, 2 to 3 times Release 6 Enhanced Uplink.

Spectrum efficiency:

– Downlink: In a loaded network, target for spectrum efficiency (bits/sec/Hz/site), 3 to 4 times Release 6 HSDPA.

– Uplink: In a loaded network, target for spectrum efficiency (bits/sec/Hz/site), 2 to 3 times Release 6 Enhanced Uplink.

Eventually, a work item was created and reached a standardization phase that was published as Release 8 in 2008. The first LTE networks were deployed in 2009 in Oslo and Stockholm by Telia Sonera, reaching data rates between 20 and 80 Mbps [17]. Unlike its predecessors, LTE was adopted rapidly in the world. By 2015, LTE subscriptions reached around 850 million worldwide [1], with 442 commercial LTE networks in 147 countries. It is expected that LTE and LTE-A will continue to grow.

Some of the novel aspects of LTE in the Radio Access Network in contrast to the previous 3GPP technologies are the spectrum flexibility and the change from Code Division Multiple Access (CDMA) to Orthogonal Frequency Division Multiple Access (OFDMA), the introduction of multiple-antenna techniques MIMO, and duplexing operation based on frequency (FDD) or time (TDD).

LTE spectrum flexibility makes it able to operate in multiple channel bandwidths, between 1.4 MHz and 20 MHz. The flexibility of the channel has made it easier for regulators around the world to determine the best bands for their countries, and carriers can continue to operate their legacy networks along with LTE. There are are currently 22 operating bands that work with LTE FDD, and 9 operating bands that work with LTE TDD.

## 2.2 LTE Frame Structure

This section will explain the frame structure in LTE and how time and frequency resources are allocated. Only the frame of LTE FDD is presented on the document, as it is the one used in this thesis.

The total duration of an LTE frame is 10 ms. Every frame is subsequently divided in 10 subframes of 1 ms, and every subframe contains 2 slots of 0.5 ms. It is important to note that the resource allocation is done on a subframe basis, i.e., the Transmission Time Interval (TTI) of LTE is set to 1 ms. Each slot can have a time duration of

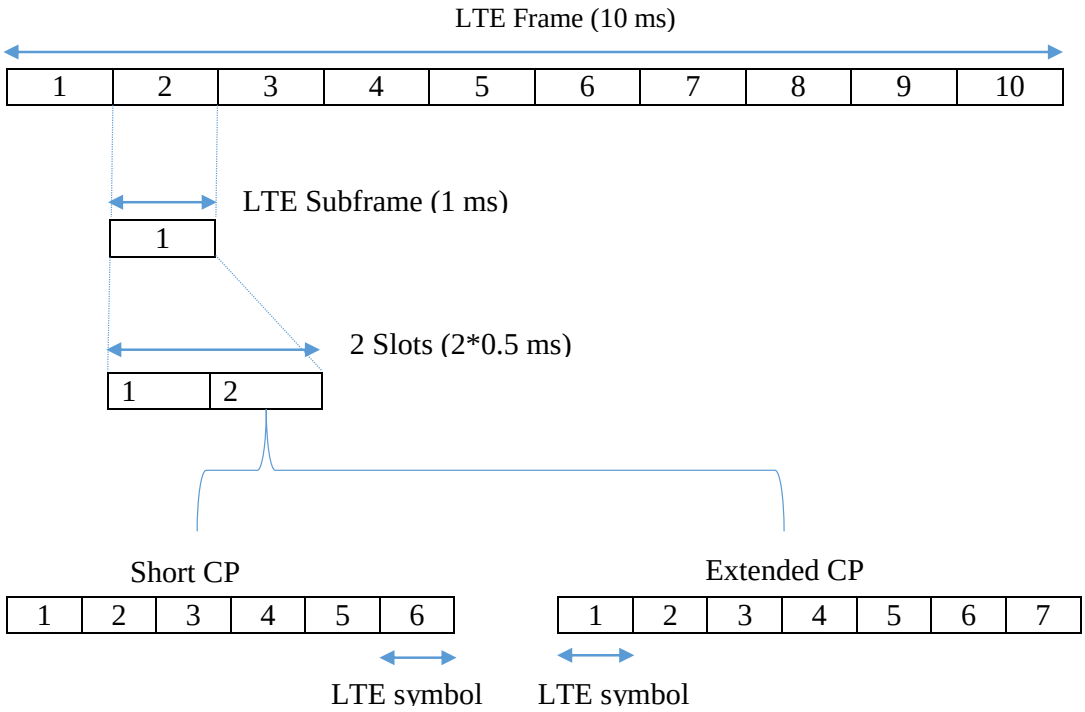


Figure 3: LTE frame structure.

either six or seven symbols, depending on the cyclic prefix used. Figure 3 shows the time structure of the LTE frame.

Cyclic prefix technique is used in order to provide robustness against Inter-Symbol Interference (ISI) created as result of multipath propagation. A copy of the last portion of the data symbol is inserted in front of the same data symbol during the guard interval. The cyclic prefix has two main purposes: it serves as a time guard against delay spread, and annexing a copy of the last portion of the symbol in front of the symbol helps keeping orthogonality among subcarriers by using linear convolution.

Resource allocation in LTE is done in frequency and time, using subcarrier blocks called Resource Block (RB). Each RB has a bandwidth of 180 kHz, consisting of 12 contiguous subcarriers and has a duration of a slot, 0.5 ms. However, the minimum resource allocation time is 1 sub frame or 2 slots (1 ms). This means, that the allocation of the second slot is implicit on the first one. Usually, when a UE is assigned a RB, it will use both RBs in the subframe. If frequency hopping is configured, the RBs carrying data for a specific UE can be in different slots. Each RB can be further divided into Resource Units, which is the duration of a symbol for 1 subcarrier. Depending on the cyclic prefix a RB consist of 84 (12x7) or 72 (12x6) Resource Units. Figure 4 portrays the two different types of RB in LTE. Table 1 provides the major physical parameters in LTE.

Table 1: LTE major physical parameters.

| | | | | | | |
|---|---|---|---|---|---|---|
| Bandwidth | 1.4 MHz | 3 MHz | 5 MHz | 10 MHz | 15 MHz | 20 MHz |
| Subframe duration | 1 ms | | | | | |
| Subcarrier spacing | 15 kHz | | | | | |
| Resource Block bandwidth | 180 kHz | | | | | |
| Number of available RBs | 6 | 15 | 25 | 50 | 75 | 100 |
| Symbols per slot | 7 with short CP, 6 with long CP | | | | | |
| Cyclic Prefix length | 5.21 µs short CP, 16.67 µs long CP | | | | | |

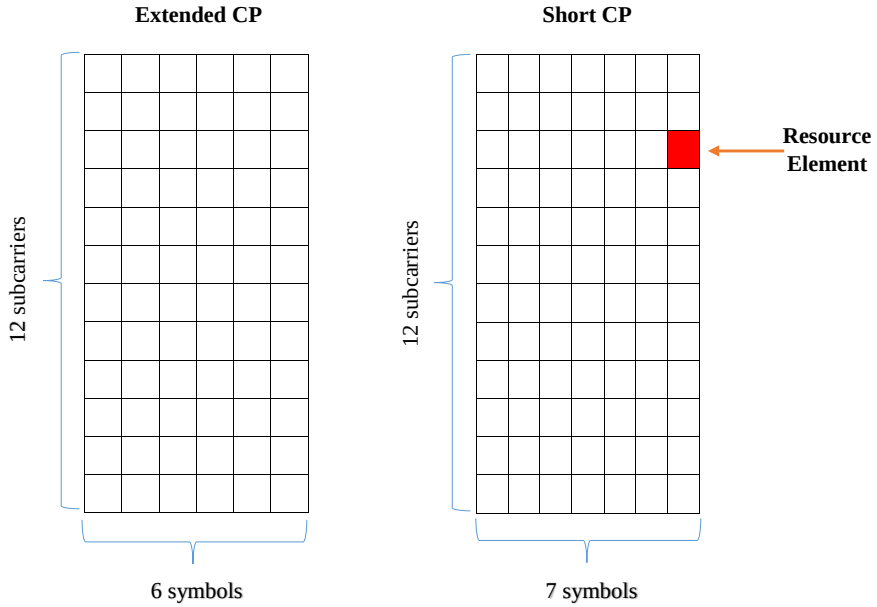


Figure 4: Two different types of RB in LTE.

## 2.3 LTE Multiple Access

LTE employs a different multiple access technique than previous 3GPP systems, such as HSDPA that employs CDMA, LTE employs OFDMA in Downlink (DL) and SC-FDMA in Uplink (UL). The following subsection will present the relevant parts of medium access in LTE that will be used in the methodology described in Chapter 3.

### 2.3.1 Downlink: OFDMA

LTE multiple access in DL, OFDMA, is based on multiple single carriers spread over a wide bandwidth channel. These single carriers called subcarriers are mutually orthogonal in the frequency domain, achieving Orthogonal Frequency Division Multiple Access (OFDMA). The premise of frequency orthogonality is that subcarriers

are separated in frequency so that at each sampling time of a desired subcarrier, all neighboring subcarriers have a zero value. Therefore, the frequency orthogonality allows more subcarriers to exist in the same bandwidth as compared to a conventional Frequency Division Multiplexing (FDM) system. The subcarriers spacing in LTE is 15 kHz, i.e., the subcarriers are spaced 15 kHz apart from each other. To maintain orthogonality, this gives a symbol rate of 66.7 µs (1/15 kHz) without CP. The extra bandwidth has a direct impact on the improved spectral efficiency and data rates of LTE. Figure 5 represents a general OFDMA system in frequency domain, it can be seen that other carriers have zero value at sampling time.

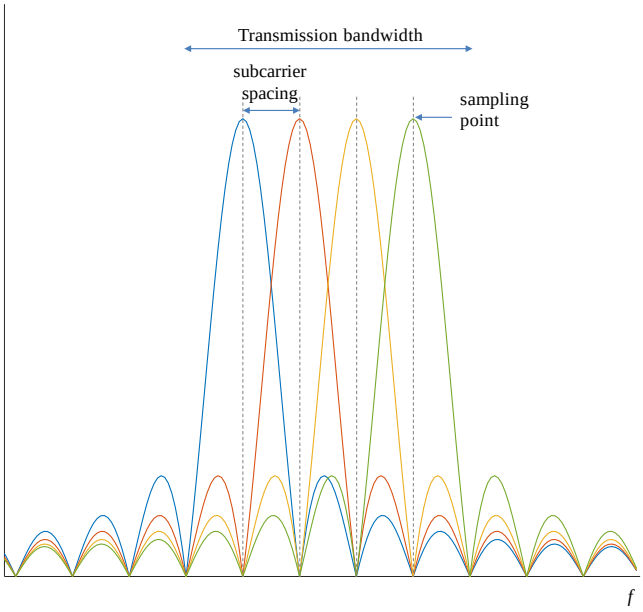


Figure 5: Representation of orthogonal carriers in the frequency domain.

The frequency orthogonality has another advantage, it mitigates the ISI caused by overlapping symbols in time and frequency domain, a common occurrence in CDMA radio systems where symbols occupy the same bandwidth. In OFDMA, because of orthogonality and the CP, the only copies that arrive in a symbol time are copies of that symbol. This simplifies the process of removing distortion in the symbol. Additionally, because of the small bandwidth channel, the subcarriers experience a flat fading channel [18]. This means that there is no need to develop complex equalizers as in the previous CDMA systems, which operate with much larger bandwidths.

Overall, OFDMA advantages in LTE can be grouped as:

- Good performance in frequency selective channels: The use of small band subcarriers helps to mitigate frequency selective channels. Channels are estimated using known reference or pilot symbols.

- Multi user and frequency diversity scheduling: OFDMA allows a dynamic resource allocation system, i.e., radio resources can be independently assigned

to users in time and frequency. The resource allocation is governed by the scheduler which in turn can implement several policies according to the operator's preference, such as opportunistic or proportional fair scheduling, among other schemes. The scheduler allocates subcarriers, grouped as RBs, to users taking into account radio channel and fading conditions. RBs assigned to a user are not necessarily contiguous in downlink. This frequency selective scheduling improves spectral efficiency and maximizes system throughput and fairness.

- Link adaptation: link adaptation is used to guarantee user data rate or QoS while maximizing system throughput [19]. LTE uses a combination of the frequency diversity scheduling, power control, and adaptive modulation and channel coding rate to meet the user requirements.

On the other side, OFDMA also has drawbacks. It is very sensitive to frequency offset (present in Doppler spread) and has a high Peak-to-Average Power Ratio (PAPR) [18]. Frequency offset can happen because of doppler spread or faulty equipment, and impacts directly on frequency orthogonality and degrades the system performance.

An OFDMA transmission in the time domain is a series of sinusoidal waves varying in amplitude in steps of 15 kHz. The dynamic nature of LTE will make the resulting signal to have a Gaussian distribution of different amplitudes [14].The varying amplitude can be overcome with high compression point power and amplifier linearization techniques [20]. For an amplifier to stay in the linear area, it will require an additional power back off. This additional power will result in a reduced power amplifier efficiency or a smaller output power. As a result, power amplifiers will have a larger power consumption for an average output power. This can be dealt on the eNodeB since it is connected to the grid, however, low power consumption is a critical aspect in mobile receivers. This is the main reason why Single Carrier Frequency Division Multiple Access (SC-FDMA) was selected as the access method in LTE uplink instead OFDMA.

### 2.3.2 Uplink: SC-FDMA

As explained in the previous section, SC-FDMA was chosen over OFDMA for uplink because of PAPR and the energy consumption it imposes on power amplifiers. SC-FDMA for LTE shares many characteristics of OFDMA: it is also divided in subcarriers of 15 kHz and allocation is done in Resource Blocks of 180 kHz. Since SC-FDMA retains the waveform characteristics of OFDMA it is not necessary to keep guard bands between users. In consequence, the sub frame of 1 ms remains the same for UL and DL. Maximum system bandwidth can also be up to 20 MHz with the same maximum number of RBs as in DL.

However, it has some differences to OFDMA, such as serial transmission, different CP, and use of timing advance as in GSM. Data in SC-FDMA is transmitted in a serial form instead of being parallel as in OFDMA [20], meaning that one symbol per user is transmitted at a time in the time domain. This allows the resulting transmission signal to retain a good signal envelope, and the waveform will be

Table 2: 3GPP requirements for LTE-A.

| Performance requirements | 3GPP requirement |
|---|---|
| DL peak spectrum efficiency | 30 bits/s/Hz (max 8 antennas) |
| UL peak spectrum efficiency | 15 bits/s/Hz (max 4 antennas) |
| DL cell edge user spectral efficiency | 0.07-0.12 bits/s/Hz |
| UL cell edge user spectral efficiency | 0.04-0.07 bits/s/Hz |
| User plane latency | 10 ms |

dominated by the modulation applied [14]. As a result, the power amplifier on the UE will operate with minimal back off, allowing a better efficiency and lowering its power consumption.

Transmission occupies a continuous part of the spectrum allocated to a user and there are no parallel waveforms transmission, hence, the diversity gain decreases with respect to OFDMA. In addition, the use of more robust modulation schemes on top of this contiguous RB involves a user's throughput reduction.

CP is not added to every symbol because of the short symbol time caused by the increase in bandwidth of the single carrier. Instead, it is added after the block of symbols which has an equal duration to a single OFDMA symbol in DL [21]. As a consequence, ISI is prevented between blocks of symbols, but not within a block. The receiver will have to use an equalizer for the block of symbols.

In order to maintain orthogonality between different carriers, transmissions need to be matched in time between each other, below the cyclic prefix duration. Otherwise, interferences between separate transmissions may occur. As a solution, timing advance is applied instead of using long guard times. In this way the eNodeB can detect the transmission from the correct frequency and time resource, as it knows which user to expect in which resource. Since this thesis is mainly focused on downlink, interested readers are referred to [22] for a complete description of LTE uplink physical layer.

## 2.4 LTE-Advanced

This section presents the main aspects of LTE-Advanced (LTE-A) that are relevant to the development of the LTE-U concept, i.e., LAA. Recall that, as mentioned before, this will take advantage of serveral existing functionalities in LTE-A as described shortly. Work on LTE-A began after the ITU-R started the process for new communication system called International Mobile Telecommunications Advanced (IMT-Advanced) in 2008 [21]. A technology approved as an IMT-Advanced technology is often considered a $4^{\text{th}}$ generation (4G) mobile system. The 3GPP submitted Release 10 LTE-Advanced and the evaluation process and specification ended in 2011.

LTE-Advanced met the IMT-Advanced requirements found in [23] and in some cases surpassed them. LTE-A requirements set by the 3GPP [24] can be seen in Table 2.

3GPP has continued to improve LTE-A with Release 11 and Release 12. In the next section some of the relevant parts of the specifications from the LTE-U perspective are presented.

### 2.4.1 Carrier Aggregation

The maximum bandwidth in LTE Release 8 is 20 MHz. This worked well for a while since most operators rarely exceeded the contiguous 20 MHz. However, the need for increased capacity and extremely high data rates has lead to the introduction of new spectrum. Although contiguous bandwidth of more than 20 MHz per operator limited the available band options [21]. The solution introduced by the 3GPP consisted in aggregating different bandwidths or carriers of 20 MHz or less, in order to increase overall system bandwidth.

This technique is referred to as Carrier Aggregation, and it is part of LTE-A Release 10 specifications. It is a band combination technology meant to improve overall system performance. As it name implies, it combines different frequency bands and use it as one virtual band. These bands may be contiguous or not, depending on the scenario. The total maximum bandwidth is extended to 100 MHz, i.e., it can support up to five different 20 MHz Component Carriers (CC). The addition of multiple carriers further extended spectrum flexibility originally planned in LTE Release 8. This flexibility may be used by operators that otherwise would be unable to access 20 MHz carriers.

CA works on 20 MHz system bandwidth and was developed to maintain backwards compatibility with LTE Release 8. CA in Release 10 is compatible with Release 8 user and control planes, including reference signals [21], resulting in a signaling overhead tradeoff for backwards compatibility. This means that a Release 8 UE can only use a single carrier, while a Release 10 and beyond UE can use the same carrier and up to 5 carriers without impacting the Release 8 UE according to the specifications. Yet, performance specification works only with two downlink CC in the first phase [21]. LTE Release 10 also included procedures such as cell management, handover control and mobility management.

There exist three different CA methods [25], represented in Figure 6 and listed below:

- Intra-band contiguous: It happens if an operator has more than contiguous 20 MHz in the same frequency band. Less likely scenario to happen because of frequency allocation conditions.
- Intra-band non-contiguous: When non contiguous carriers are available to an operator in a frequency band and are aggregated.
- Inter-band non-contiguous: The carriers are on different frequency bands and are aggregated. Radio propagation characteristics of different frequency bands must be considered and may even be exploited. This feature can be used for integrated the targeting unlicensed bands in LAA.

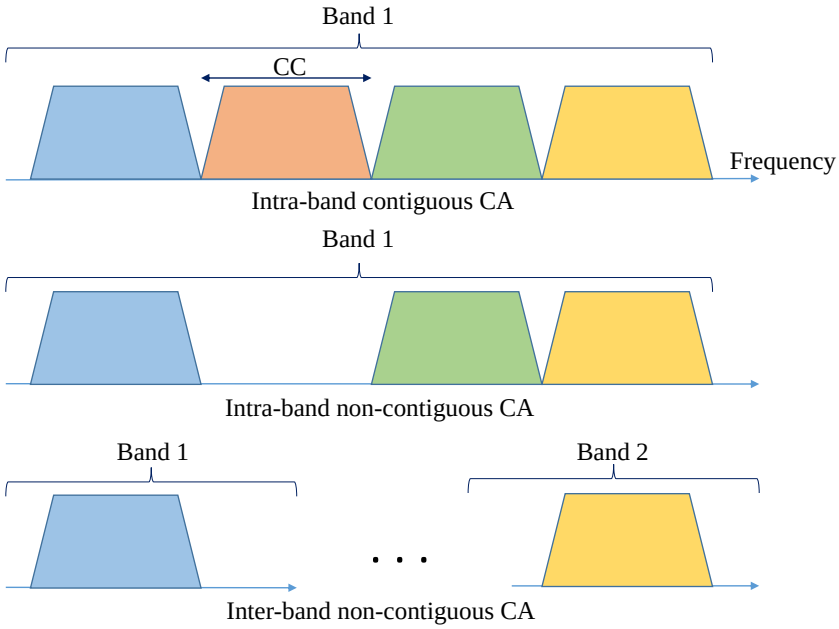


Figure 6: Types of Carrier Aggregation.

In addition to these methods, there are mainly four deployment scenario for CA [26], represented in Figure 7:

- Scenario 1: CCs are overlaid in the same frequency band. Coverage is nearly the same.
- Scenario 2: CCs are overlaid in different frequency bands. Coverage is different due to different path loss, where the CC with higher frequency is used for CA.
- Scenario 3: CCs are overlaid in different frequency bands using different beam directions or patterns between each other. F2 is directed to cell edge of F1, thus improving throughput at cell edge.
- Scenario 4: One CC will provide macro coverage on a lower frequency, several Radio Remote Head (RRH) units will use a higher frequency to offload traffic in hotspots.

As the reader may infer, Scenario 2 and 3 nicely fit the philosophy behind LTE in unlicensed spectrum. Indeed, Scenario 4 is very likely to be an LAA deployment model for indoor, where dedicated LTE-U or LAA access points can be 1) deployed as required, 2) controlled by a cloud-RAN [27], and 3) connected to a closer macrocell.

The advantages of CA include load balancing, resource sharing, increased frequency diversity scheduling, and higher peak data rate. Basically, the scheduler now has a shared pool of resources from the different frequencies, resulting in more options of available RBs for every UE. The increased amount of RB over different frequencies, and therefore different path loss, makes it more likely to find RBs with a better SINR that will allow a higher order modulation and ultimately higher data

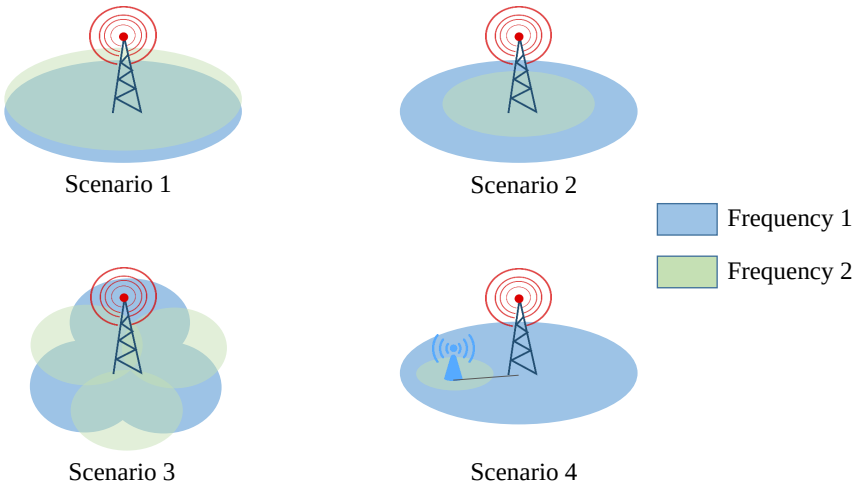


Figure 7: Carrier Aggregation deployment scenarios.

rates. The pooled resources makes the scheduling less sensitive to momentary uneven loads on the network and will increase peak data rates when the load on the network is low [21].

The introduction of CA in LTE Release 10 is not without challenges and future improvements. The increased signaling overhead as a result of backwards compatibility with Release 8 can be further improved, and the need for more complex CA-capable terminals with new functionalities and higher power consumption are key tradeoffs to be taken into account [30].

Summarizing, Carrier Aggregation provides various benefits as higher data, increased spectrum flexibility and efficiency, while maintaining backwards compatibility with LTE Release 8, reducing implementation and specification complexity. Challenges in CA include energy consumption, reducing signaling overhead and increased receiver complexity. Nevertheless, CA is expected to become popular since its benefits outweighs by far the drawbacks, and more important, it is a key feature to extend the benefits of LTE to the unlicensed spectrum..

## 2.5 Virtualization techniques

Virtualization techniques became relevant to operators, as they need to satisfy increasing service demand and generating profit, even as the cost per bit levels are falling and users expect lower fares. Novel solutions that aim for more flexible resource management, advanced self-organization and dynamic configuration are Software Defined Network (SDN), Network Function Virtualization (NFV) and Cloud Radio Access Network (C-RAN) [28]. These three technologies are related, but contribute for different domains [3], and can work independently from each other.

- **Software Defined Network (SDN)**: SDN is a new network architecture that aims to decouple the control plane from the data plane of the infrastructure equipment [29]. The decoupling is achieved via software controllers which in

turn are logically centralized. One of the main advantages of this architecture is that solutions are not multi vendor-specific anymore. As a result of the global view of the network, resource management can be dynamically adjusted or automated by SDN programs [3].

- **Network Function Virtualization (NFV)**: NFV is the implementation of network function in software running over general purpose computing platforms [30]. This implies virtualization techniques of network equipments from hardware specific technology to standard high volume servers, switches and storage. The main motivation for NFV is to reduce the life and innovation cycles of mobile networks through software updates rather than hardware updates [3]. Additionally, and no less important, equipment costs and power consumption are reduced through the flexibility and scalability of the IT industry.

- **Cloud-RAN (C-RAN)**: Also called Centralized-RAN, it is a new cellular network architecture base on cloud computing. The reasoning behind it is to separate the Baseband Units (BBU) from the radio access units [27]. The BBUs are centralized in a virtualized pool of resources using cloud computing. This will alleviate the processing load of base stations while keeping high bandwidth and low latency links. The radio access units are known as Radio Resource Heads (RRH) are less complex and have lower energy consumption, making them easier for deployment and scalability [3].

  As with SDN and NFV, the centralized use of resources enables an efficient usage of BBUs, and reduces the costs associated with cell deployment and operation [27]. A very important possibility of of C-RAN is the implementation of efficient interference avoidance and cancellation algorithms in multiple cells by selectively turning RRHs, as well as Cell Switch Off (CSO) schemes [31], according to traffic fluctuation in different scenarios [3].

These three technologies are motivated by the need for dynamic and automated configuration and scalability of network and radio resources as service demand is highly time-varying and diverse, and hence, it is important to achieve the highest possible efficiency and to avoid idle resources. Although these technologies have their own respective challenges, centralized processing and virtualization techniques in the Core Network with SDN and NFV, and the Radio Access Network with C-RAN, they are expected to reduce the overall cost of the networks and help operators to deal with the increasing demand of current and future mobile networks.

As it will be shown in later sections, the framework investigated in this thesis can benefit from these solutions.

## 2.6 LTE in unlicensed spectrum

As previously explained, several aspects have motivated the development of LTE in unlicensed spectrum: the possibility of using CA, advent of small cells, necessary high data rates in the near future, and the time and cost of allocating new free spectrum for mobile communications.

As an example, in the USA, The Federal Communications Commission (FCC) has released several unlicensed bands for commercial use, mainly the industrial, scientific and medical (ISM) band in 2.4 GHz, the unlicensed national information infrastructure (U-NII) band in 5 GHz, and the millimeter-wave (mmWave) band in 60 GHz.

The 5 GHz band has many aspects that make it attractive for LTE deployment. It has relatively good channel propagation for mobile networks [7], and wide spectrum available [8]. As a result, the 5 GHz band became the *de facto* band for any research for LTE in unlicensed spectrum.

### 2.6.1 Regulations in the 5 GHz band

The growing interest and development of LTE in unlicensed spectrum has been followed by regulatory agents, organizations, the media, and the industry among other stakeholders [32], [33]. Special attention has been brought to coexistence with other RATs and systems, specially WiFi. Therefore, it is important to study the regulatory requirements in the band, and the different stakeholders to be aware or cooperate with the development of the different LTE in unlicensed spectrum products.

LTE in unlicensed spectrum over the 5 GHz band, as any other RAT in the same band, has to comply with different regulations to ensure a proper coexistence with other systems. These regulations include transmission power, channel access method, spectral density, channel bandwidth, out of band emission, etc. A complete overview of regulations throughout the world can be found in [34] and [8].

Among these regulatory requirements, the more relevant for coexistence are transmission power, channel selection and clear channel assessment [4].

Transmission power in unlicensed spectrum is often regulated as an interference management method, and the 5 GHz band is no exception. For example, US regulations allow for a maximum of 30 dBm, or 1 W, peak output power. In Europe, the maximum power transmission in RLAN designated bands is also 30 dBm. The transmission power regulation directly impacts the potential deployment scenarios of LTE in unlicensed spectrum. Usually, LTE macro cells have a maximum output power well over 40 dBm, whereas 30 dBm is more common in small cells. This makes LTE-U ideal for deploying small cells and indoors, where low range is expected.

Proper channel selection is a key regulation in Europe and US, and in other nations. Meteorological radars operate in the 5 GHz band, and regulations are enforced to keep other systems from interfering on them. As a result, a method known as Dynamic Frequency Selection (DFS) was created as an interference avoidance mechanism. DFS forces devices in the same band to detect if a radar signal is being transmitted. If a radar signal is detected, then the device will switch to a channel that is not interfering with the radar. According to ETSI specifications [34], DFS mechanism should be able to detect signals above a threshold of –62 dBm for devices with a maximum EIRP of 200 mW, and –64 dBm for devices with a maximum EIRP 1 W.

Lastly, Clear Channel Assessment (CCA) is a principle that ensures that existing RATs confirm the channel is idle before transmission; CCA procedure is commonly

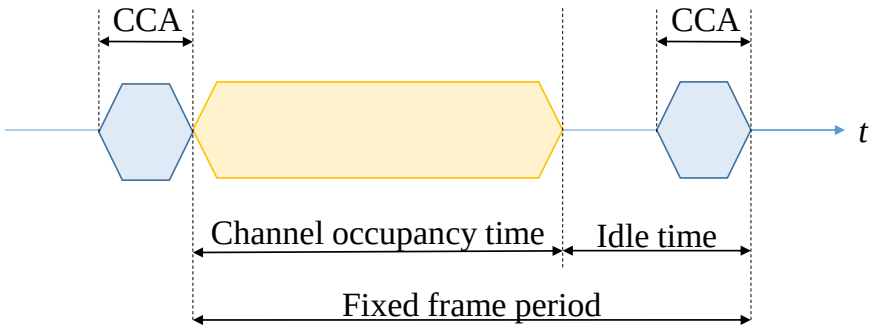


Figure 8: LBT specification for frame based equipment according to ETSI [35].

referred as listen-before-talk (LBT) [4]. European, Japanese, and Indian regulations mandate the usage of LBT in the unlicensed bands, whereas United States, China, and South Korea don't require it.

When a device following LBT procedure is ready for transmission, it will listen to the channel for a period known as clear channel assessment period, and will at least utilize energy level detection to determine the presence or absence of other signals in order to determine if the channel is occupied or clear. The device is allowed to transmit only if the energy level is below a preset threshold value.

In addition, certain regions such as Europe and Japan prohibit continuous transmission and impose limits on the maximum duration of a transmission burst in the unlicensed spectrum. ETSI specifications [35] allow for a maximum channel occupancy time of 10 ms, and a CCA period of 20 µs. The time frame of ETSI specification is seen in Figure 8.

The maximum channel occupancy time will result in a discontinuous transmission in LTE, and therefore making LTE in unlicensed spectrum performance time varying and dependent on other systems. This expected drop in performance will result in tradeoff to be made in order to use unlicensed spectrum.

Besides LBT, other proposals for coexistence have been introduced: the use of duty cycles and dynamic channel selection schemes similar to the ones currently used in WiFi systems.

### 2.6.2 Coexistence with WiFi

One of the main challenges is a fair coexistence between LTE in unlicensed spectrum with other communication systems, specially with WiFi. The coexistence with WiFi is of utmost importance due to the major role WiFi plays in current wireless networks. By 2017, an estimated 7 billion of WiFi enabled devices will be in use [36], from residential networks to small business, enterprise, and carrier grade networks.

Since LTE was developed as a stand-alone network with spectrum efficiency and interference management, there are justified concerns that LTE could take over of the 5 GHz band [32], [33]. Furthermore, WiFi performance degradation caused by LTE operating in unlicensed spectrum at its current state has been thoroughly researched

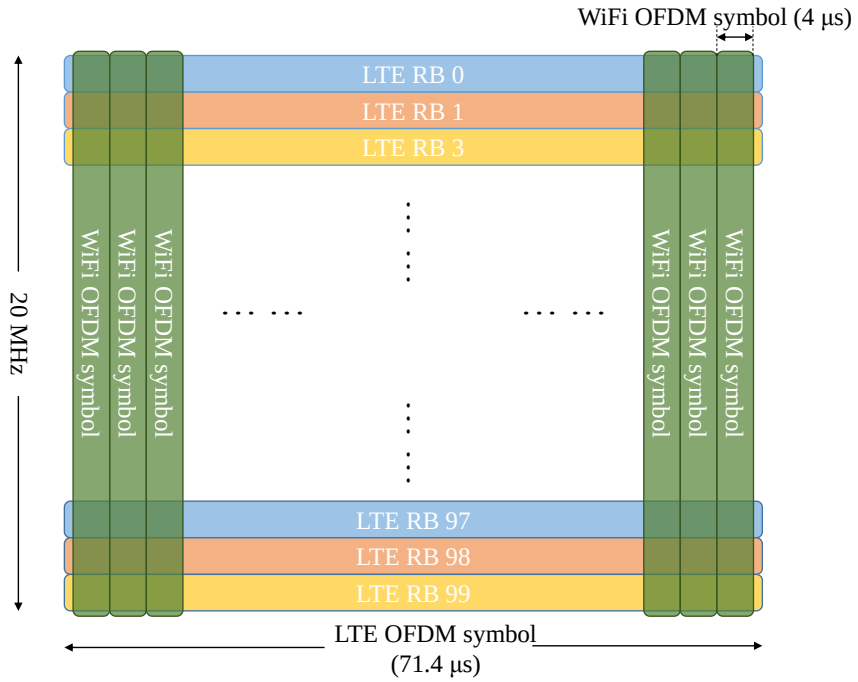


Figure 9: Frequency and time comparison between LTE and WiFi symbols [37].

in recent years [10] [11] [12]. It has been shown that LTE will use all the spectrum available and will not fairly coexist with other systems.

The reason behind the WiFi performance degradation when LTE is present lies on WiFi's media access. WiFi channel access mechanism is known as distributed coordination function (DCF), a contention based protocol known as carrier sense multiple access with collision avoidance (CSMA/CA). CSMA/CA is a decentralized protocol where nodes listen to the channel prior to transmission to ensure clear channel assessment, i.e., WiFi always uses LBT. A node or device in a WiFi network during CCA period, i.e., LBT may receive transmissions from other nodes or RATs, causing the channel to be seen as occupied. The device will avoid a collision and will halt its transmission for a period of time before sensing the channel again. This period of time is exponential in WiFi and it serves as a collision avoidance mechanism when more than one device sense the medium idle at the same time. Essentially, CSMA/CA, and therefore DCF, results in a tradeoff between a low collision probability and a lower channel utilization as more users want to use the channel.

WiFi and LTE also differ in the physical layer features. LTE employs OFDMA subcarriers grouped as RBs over the system bandwidth, with scheduling advantages such as a multi user and multi frequency diversity described in section 2.3.1. On the other side, WiFi employs a TDD scheme where the whole system bandwidth is taken by a user at a time, either in DL (the access point) or UL (users). This in turn impacts the symbol period making it shorter than an LTE symbol. The different features can be seen in Figure 9. These differences between LTE and WiFI physical layer and media access are being addressed in the development of LTE in unlicensed

spectrum to ensure a fair coexistence with WiFi and other RATs. However, it worth saying that they also complicate the development of accurate models to study the performance and coexistence of both systems.

### 2.6.3 Current research

The industry and academic proposals for LTE in unlicensed spectrum will be covered in the next section.

At the moment, the three main branches of LTE in unlicensed spectrum in the industry are: LTE License-Assisted Access (LAA), LTE-Unlicensed (LTE-U) and MulteFire. LTE LAA is being developed by 3GPP and is expected to be included in LTE Release 13. LTE-U is being developed by the LTE-U Forum, a consortium of private companies including Ericsson, Samsung, Qualcomm and Verizon. The third branch, MulteFire differs from LTE LAA and LTE-U and is being developed by Qualcomm, Nokia and others in the MulteFire alliance.

#### LTE LAA

LTE LAA is being standardized by 3GPP and the specifications are expected to be in Release 13 in 2016. The range of operation for LTE LAA is defined between 5150 MHz to 5925 MHz .

The main concept in licensed assisted access deployment is to use CA between licensed and unlicensed bands. Initially LAA will be deployed as supplemental downlink (SDL), and it will follow the specification of ETSI for unlicensed spectrum. In LTE LAA a user is configured with a primary cell (PCell) in the licensed band and one or more secondary cells (SCells) in the unlicensed band. The PCell will always remain on the licensed band, serving as the anchor for the Scell in the unlicensed band, hence the name Licensed-Assisted Access.

3GPP's aim with LAA is to develop a single global solution framework, in other words, a framework that would work with every regulation. 3GPP emphasizes that unlicensed spectrum can not match the quality of licensed spectrum, neither can it satisfy the need of more licensed spectrum because of its inability to be used in macro cells providing wide-area coverage due to uncontrolled interference [8].

Based on small cells on carrier aggregation, 3GPP has developed four possible small cell deployment scenarios for LAA, fully described in [8]. They can be seen in Figure 10 and table 3.

Based on the scenarios and regulations, the following functionalities are required for an LAA system:

- Listen-before-talk.
- Discontinuous transmission on a carrier with limited maximum transmission duration.
- Dynamic frequency selection for radar avoidance.
- Carrier selection.

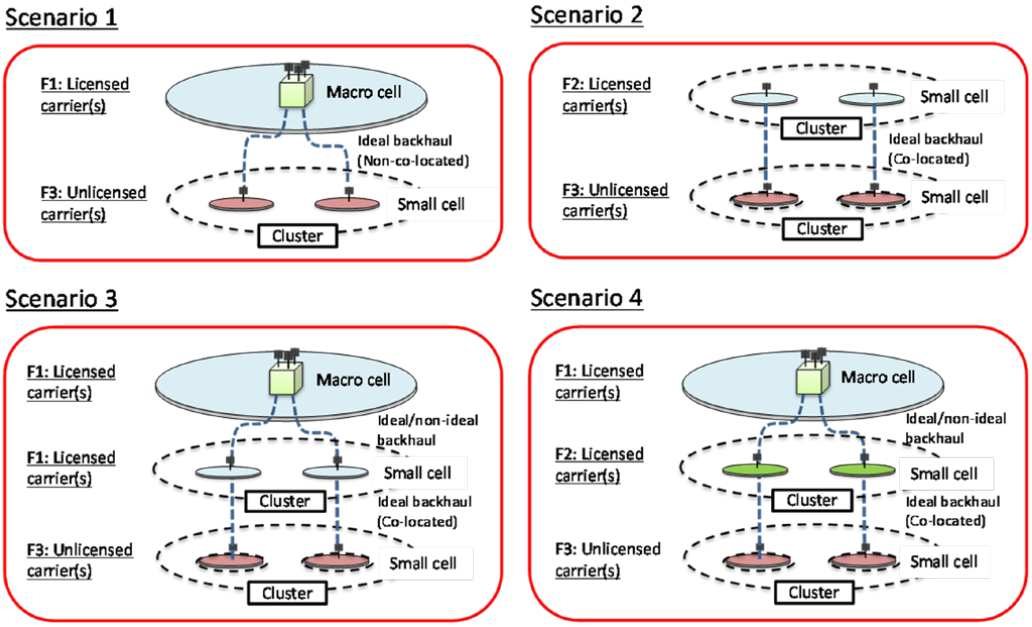


Figure 10: Different LTE LAA deployments

Table 3: LTE LAA deployment scenarios

| | |
|---|---|
| Scenario 1 | Carrier aggregation between licensed macro cell (F1) and unlicensed small cell (F3). |
| Scenario 2 | Carrier aggregation between licensed small cell (F2) and unlicensed small cell (F3). |
| Scenario 3 | Licensed macro cell and small cell (F1) with carrier aggregation between licensed small cell (F1) and unlicensed small cell (F3). |
| Scenario 4 | Licensed macro cell (F1), licensed small cell (F2) and unlicensed small cell (F3):<br>-Carrier aggregation between licensed small cell (F2) and unlicensed small cell (F3).<br>-Carrier aggregation between macro cell (F1), licensed small cell (F2) and unlicensed small cell (F3) if there is ideal backhaul between macro cell and small cell.<br>If dual connectivity is enabled, there can be dual connectivity between macro cell and small cell. |

- Transmit Power Control.
- Radio Resource Managment (RRM) measurements including cell identification.
- Channel-State Information (CSI) measurement.

Another key design target is the fair coexistence with WiFi networks, where LAA should not impact WiFi performance more than an additional Wi-Fi network on

the same carrier. LBT is the method chosen by 3GPP to ensure a fair coexistence between LAA and any other RATs, and it is being developed in compliance with ETSI regulations. For the coexistence evaluation study, 3GPP expanded the way LBT is implemented for media access, it considered four different categories.

The evaluated channel access schemes can be classified into the following categories:

- Category 1- No LBT: No LBT procedure is performed by the transmitting entity.
- Category 2- LBT without random back-off: The duration of time that the channel is sensed to be idle before the transmitting entity transmits is deterministic.
- Category 3- LBT with random back-off with a contention window of fixed size: The transmitter draws a random number N within a contention window. The size of the contention window is specified by the minimum and maximum value of N. The size of the contention window is fixed. The random number N determines the duration of time that the channel is sensed to be idle before beginning transmission on the channel.
- Category 4- LBT with random back-off with a contention window of variable size: The transmitter draws a random number N within a contention window. The size of contention window is specified by the minimum and maximum value of N. The transmitting entity can vary the size of the contention window when drawing the random number N. The random number N determines the duration of time that the channel is sensed to be idle before beginning transmission on the channel.

The technical report of LAA [8] includes coexistence evaluation results with WiFi and other LAA operators. The results are summarized in table 4.

Table 4: Coexistence evaluation results between DL-only LAA and WiFi

| Channel access | Evaluation results |
|---|---|
| LBT Category 1 | An LAA network cannot operate without impacting Wi-Fi in at least some performance metrics. |
| LBT Category 2 | An LAA network can operate without impacting Wi-Fi more than an equivalent Wi-Fi network. |
| LBT Category 3 | An LAA network with modifications including at least a defer period can operate without impacting Wi-Fi more than another Wi-Fi network. |
| LBT Category 4 | An LAA network with modifications including at least defer periods and variable (exponential) contention windows can operate without impacting Wi-Fi more than an equivalent Wi-Fi network. |

The report also included an adjacent channel interference test, where it was proven that LAA and Wi-Fi can coexist in adjacent channels. According to 3GPP,

LAA causes less adjacent channel interference to a Wi-Fi system compared to another Wi-Fi system.

Based on the coexistence results, 3GPP recommended a category 4 LBT scheme including random back off and variable contention windows as a baseline for LAA downlink data transmissions. 3GPP also recommended configurable limits on the random backoff time and contention window size to ensure a fair operation in unlicensed spectrum.

**LTE-U**

LTE-U is along with LAA, the front runners of LTE in unlicensed spectrum. It is being developed by the LTE-U Forum, a a private group effort formed by Verizon, Alcatel-Lucent, Ericsson, Qualcomm and Samsung in 2014. LTE-U Forum aims to develop LTE-U in order to deploy it in a short amount of time in markets where LBT is not a regulatory requirement such as US, China and Korea.

LTE-U as LAA is being developed to work as Supplemental Downlink using Carrier Aggregation. However, unlike LAA, LTE-U is not being developed as a global framework, it is targeted primarily for the US instead. LTE-U is in compliance with US's FCC regulations, and the specifications planned for LTE-U will support LTE in the 5 GHz UNII-1 and UNII-3 bands [38].

Fair coexistence between LTE-U and WiFi as well as between LTE-U operators is also one of the most important objectives for LTE-U. Yet, the approach used by LTE-U is different from the one used by 3GPP. Unlike LTE LAA, LTE-U coexistence approach doesn't rely on clear channel assessment, instead it will use an access method called carrier-sensing adaptive transmission (CSAT), specified in [39].

The idea behind CSAT is to define a duty cycle based on the amount of networks present to determine media access. During this duty cycle, the LTE-U small cells will alternate between on and off transmission styles. When data is being transmitted through the SCell it is referred as SCell ON-state and when it is not being used, it is referred as SCell OFF-state. During the SCell ON-state, the eNodeB broadcasts LTE-U Discovery Signals (LDS) in order to keep the LTE-U UE synchronized in time and frequency, and for the UE to perform tracking and measurements of the SCell. LDS are transmitted periodically regardless of the amount of users in the SCell.

The cycle ratio between on and off can be adaptively adjusted depending on the channel activity sensed during the SCell OFF-state. During this period, other LTE-U or WiFi nodes are sensed if they are above the CCA Energy Detection level of -62 dBm. The minimum SCell OFF-state duration time is of 1 ms, while the maximum SCell OFF-state duration time is defined by the LDS periodicity, which can vary between 40 ms, 80 ms, or 160 ms. CSAT duty cycle may have a long sense period to ensure proper sensing, however, this long sense period may result in a perceived delay experience on the end user [4].

The SCell ON-state has a minimum duration of 4 ms as long as there is data to transmit. LDS are also included in SCell ON-state and its transmissions can be 1 ms long. SCell ON-state has a maximum duration is of 20 ms, in order to ensure a fair channel coexistence.

LTE-U Forum conducted coexistence evaluation in [38], [40] for DL only LTE-U using 3GPP LTE Release 10 onwards. They concluded that the in a WiFi deployment where one of the nodes is replaced by a LTE-U node, the remaining WiFi nodes performance is no worse than before, and in some cases it improves.

While LTE-U Forum has claimed positive coexistence results, reception from the industry has been mixed. The main criticism for LTE-U is that it is not being developed by a known standards organization, but by private effort and without open collaboration from other stakeholders [32]; and that it will disrupt WiFi since it does not use LBT. In light of the increasing concern, LTE-U Forum and Wi-Fi Alliance started a series of activities as workshops, simulations, and coexistence testing guidelines to procure a fair coexistence [41]. LTE-U Forum is expected to begin tests in Verizon facilities during 2016, and the FCC has a released a statement [42], where it expects a continued cooperation of all of the stakeholders for a resolution of spectrum sharing concerns.

### MulteFire

A third effort to develop LTE in unlicensed spectrum is MulteFire, a device family originally developed by Qualcomm. It is now being developed under the MulteFire Alliance, including members as Qualcomm, Nokia, Ericsson, and Intel.

MulteFire main goal is to completely deploy a stand alone LTE network in unlicensed spectrum, where the devices deployed would be akin to a current WiFi Access Point. MulteFire could be deployed by cable companies, Internet Service Providers, small businesses, enterprises, venue owners, building owners and mobile operators [43].

MulteFire would combine the advantages of WiFi deployments with the robust radio link performance of LTE. MulteFire should be specially helpful in indoor scenarios and in hyper dense environments [43].

MulteFire represents an innovation on spectrum for LTE in mobile networks, where mobile carriers licensed spectrum advantage would be diminished by new players using unlicensed spectrum.

However, MulteFire technical information is not easily available. Although MulteFire has pledged similar coexistence objectives as LTE-U and LAA, no coexistence or performance evaluation studies have been published by Qualcomm or the MulteFire Alliance. Using the current information available, it is not possible to determine whether MulteFire will fulfill its claims of fair coexistence over unlicensed spectrum.

### Other Research

Several other alternatives have also been proposed either for LAA or LTE-U or as independent research for LTE in unlicensed spectrum. These proposals can be classified in four different categories:

- Dynamic Channel Selection (DCS): where the focus is to find a free channel.
- Listen-Before-Talk (LBT): where a Clear Channel Assessment is needed before using the channel.

- Duty Cycle (DC): where the channel is used and released periodically.
- Power Control (PC): where transmit power is adjusted.

Most of the related work focuses on performance assessment and mechanism to improve the coexistence with WiFi and other systems by using combination or variations of the aforementioned categories. The alternatives vary greatly, going from analytical models, measurements, and experimental settings. Table 5 provides a summary of some recent contributions.

Even when the development of LTE in unlicensed spectrum is relatively new, it has been approached by different angles. This thesis takes a different approach: **network planning and radio access optimization**. Despite the current work on coexistence schemes with WiFi and other RATs, network planning and radio access optimization remain as complementary powerful tools for the correct operation of LTE in unlicensed spectrum. This approach is presented in the framework described in detail in Chapter 3 and Chapter 4.

Table 5: Summary of related work.

| **Ref.** | **Test case** | **Scheme** | **Method** |
|---|---|---|---|
| [44] | LTE-U/WiFi: Indoors | DC + PC | S |
| [4] | LTE-U/WiFi: HetNets | DC | S |
| [45] | LTE-U/LTE-U: Outdoors | DC-based | S |
| [46] | LTE-U/WiFi: Outdoors | DC + PC | S + A |
| [47] | LTE-U/WiFi: Both | DCS + PC | S + A |
| [48], [49] | LTE-U/WiFi: Both | LBT-based | A |
| [50] | LTE-U/WiFi: Indoors | DCS-based | S + A |
| [51] | LTE-U/WiFi: Both | LBT-DCS | S + A |
| [52] | LTE-U/WiFi: Indoors | PC | S |
| [53] | LTE-U/WiFi: Indoors | DC + LBT | A + S |
| [54] | LTE-U/WiFi: Indoors | DC-based | A |
| [55] | LTE-U/WiFi: Indoors | LBT | E |
| [56] | LTE-U/WiFi: Indoors | DC-based | S |
| [37] | LTE-U/WiFi: Indoors | LBT-based | S |

S: Simulations; A: Analytic; E: Experiments

## 2.7 Remarks

This chapter has presented an overview of LTE, the elements of LTE that are relevant in the development of LTE in unlicensed spectrum, as well as a state of the art in LTE in unlicensed spectrum. The focus is limited only to the physical and data link layer, where upper layers and network architecture are omitted.

LTE characteristics, such as its media access, coding and scheduling, make it highly resistant to interference while offering high data rates at the same time. However,

these very characteristics cause the development of LTE in unlicensed spectrum to be challenging, since it was designed as a RAT that would take full advantage of the available system bandwidth. This greedy behavior of LTE contradicts the *ethos* of unlicensed spectrum, i.e. fair and friendly use of the spectrum. A vital part of the success of LTE in unlicensed spectrum depends in how well it will coexist with other RATs, specially with WiFi; as WiFi is certainly on the most famous and extensively deployed RAT in the world.

Additionally, the 5 GHz band became the *de facto* band for any research on unlicensed spectrum. Transmission power regulations of the 5 GHz band, along with its higher frequency as current LTE bands make the LTE in unlicensed spectrum ideal for small cells and indoor scenarios, where the largest amount of data is transferred.

Three main research brands of LTE in unlicensed spectrum were reviewed: LTE LAA, LTE-U, and MulteFire. LAA and LTE-U branches are based in an inter-band non-contiguous CA, while MulteFire is planned to be a stand alone deployment. LTE LAA, developed by 3GPP, is regarded to be the front runner of the three and it will constitute a global solution following coexistence via LBT; its standard specifications will be ready available for LTE Relase 13 in 2016. On the other hand, LTE-U is regarded to be very US-centric, following closely FCC's regulations, with a different approach to coexistence based on duty cycle instead of LBT.

Finally, it is worth applying new virtualization technologies, such as SDN, NFV, C-RAN to LTE in unlicensed spectrum. These are expected to reduce the overall cost of the networks for operators and to adapt to the increasing demand of current and future mobile networks.

# 3 Proposed Framework

Chapter 1 and 2 helped to explain the background necessary to understand the development of LTE in unlicensed spectrum, hereafter LTE-U[1], and its relevance in the mobile networks industry. This chapter explains in detail the contribution of this thesis, the proposed framework.

As it was briefly explained in the introduction, the framework presented is focused on network planning and radio access optimization. More specifically, the deployment of LTE in unlicensed bands in indoor environments is investigated. In this context, radio access planning is the main tool to determine the number of nodes and their locations to satisfy a certain service demand. This is carried out by means of a statistical model that captures the behavior, performance, and coexistence of two wireless technologies (LTE-U and WiFi). A high level design representation of the proposed framework is shown in Figure 11. It is composed of 5 stages, or modules:

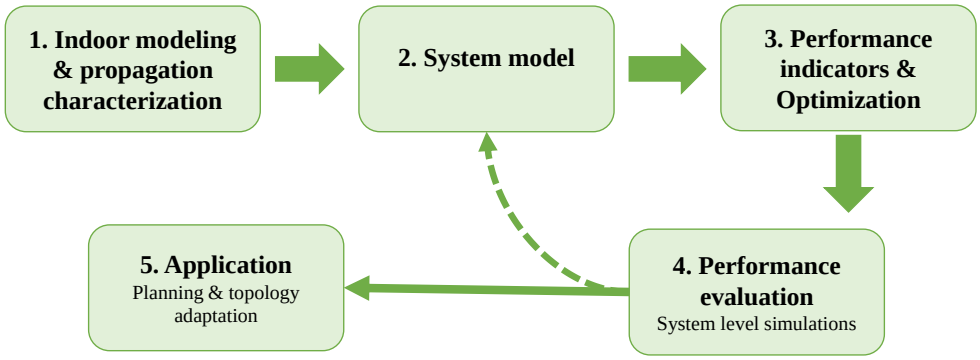


Figure 11: Proposed framework for the thesis.

1. **Indoor modeling and channel propagation characterization**: 3D modeling techniques are used for accurately represent the indoor environment, and deterministic methods (RT) are used to characterize the radio propagation.

2. **The system model**: a set of mathematical objects to model in statistical terms, yet as accurate as possible, the behavior and performance of both systems.

3. **Performance indicators & optimization**: a set of performance indicators, service specific demands, and constraints are configured. Then, optimized network topologies are obtained using multiobjective optimization methods.

4. **System-level simulations (SLS)**: simulations are run in order to validate the performance of the optimized network topologies. This stage is also used as feedback for stage 2 in order to correct any error and improve the system model.

[1]Abbreviated for the sake of readability, and in no relation whatsoever to the RAT developed by LTE-U Forum

5. **Application**: The end result of the optimization and system-level simulations can be directly used for indoor planning or radio access optimization.

This chapter is organized as follows: Section 3.1 will explain in detail the indoor environment and channel characterization. Section 3.2 introduces multi objective optimization and the evolutionary algorithm used for the indoor planning optimization. Finally, section 3.3 introduces the concept of system-level simulation and the simulations used in this thesis. Due to their importance, the system model used and the optimization problem formulation will be explained separately in Chapter 4.

## 3.1 Indoor environment and channel characterization

Indoor channel propagation corresponds to the first stage of the proposed framework. This stage can be divided in two steps: the indoor environment modeling, and the channel characterization, or propagation prediction. These sub stages are related since a reliable channel characterization is dependent on a correct indoor environment model.

### Indoor environment model

The representation of indoor environments is a fundamental step in the deployment and analysis of any indoor wireless system, where predicting the received signal strength may be critical for the performance of the radio link. The nature of this study is based in indoor environments, hence it is essential to consider the particularities of the indoor environments: actual structures, layouts, and materials. The near infinite combinations of these elements and their effects on radio propagation, such as severe multipath and shadowing, make the modeling of indoor environments challenging and in many times case-specific.

In the light of these necessities, 3D models and databases are popular tools that help us to integrate the necessary information of indoor environments. This study utilizes a 3D model and database developed by the software program WallMan, a software included in WinProp software package developed by AWE Communications. Wallman creates a graphical user interface that allows to edit the 3D model and the indoor database. This database contains the information of all the wall segments in the building, as well as the three-dimensional location of its corners, and the information of the material of each wall segment.

The indoor database information of WallMan and other similar tools contains relevant information to estimate the propagation of electromagnetic waves, such electrical characteristics of different materials at different frequency ranges. Thus, this information helps the model to be as close as possible to the real life scenario.

The building selected for the study in this thesis is the Aalto University School of Electrical Engineering located in Otakaari 5, Espoo. The development of the indoor database and 3D model of the building, seen in Figure 12a, is previous to this thesis, and was performed by the department of Communications and Networking. The building has an irregular shape which can be seen in Figure 12b, where a main hallway connects the different wings, the lobby, and the lecture halls. It has a selection of

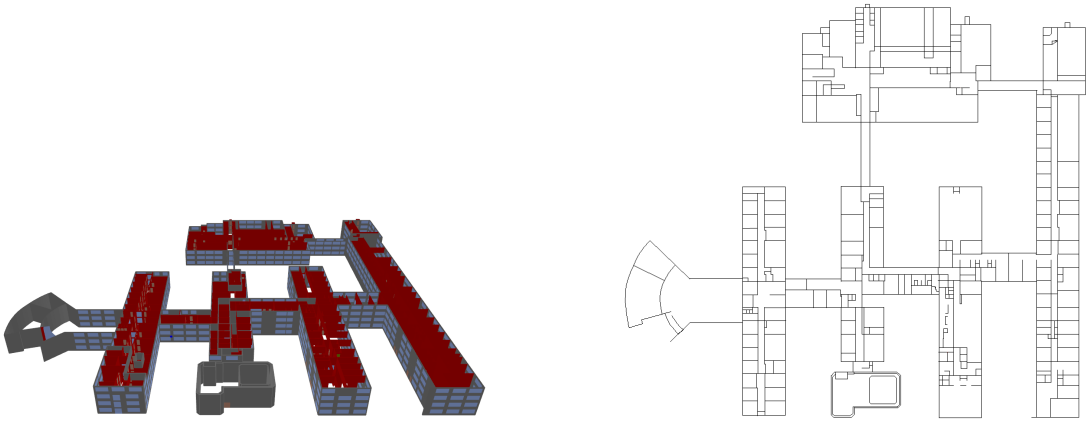

(a) 3D model. (b) Building layout.

Figure 12: Building map and 3D model.

lecture halls, offices, hallways, and rooms of different sizes. Different materials are used throughout the building, lecture halls and inner rooms have concrete walls, offices and hallways have a mixture of brick walls and double pane glass windows.

The aforementioned characteristics create a complex layout of the building which directly affects the properties of electromagnetic waves, such as reflection, diffraction and penetration losses. Summarizing, the building's complex shape, rooms and materials provide a sufficiently vast scenario to study a mobile network.

In addition, the building spaces are occupied differently during the day and throughout the building. For example, user density in spaces like the cafeteria and lecture halls can increase drastically in a short amount of time, creating an uneven service demand in the building. This uneven service demand will be exploited on the system model and SLS in Chapter 4 and Chapter 5, respectively.

### 3.1.1 Indoor channel characterization

This section explains the method used for the indoor channel characterization, the reasons why it was used as compared to other known methods and also a concise explanation of channel modeling.

The method selected for the indoor channel propagation prediction in this thesis is called Ray Tracing (RT). Ray Tracing is a deterministic method that takes advantage of the details contained in 3D models and databases. Yet, in order to fully understand the reason behind the decision of using RT, it is necessary to review the behaviour of the wireless channel and the different kinds of models available to represent it.

Wireless communications system operate by transmitting electromagnetic waves over the air interface on what is usually known as the wireless channel, radio channel or just the channel. The wireless channel presents a crucially different behavior than its wired counterpart, as it experiences strong variations over time and over frequency.

These different kinds of variation, or fading, can be classified into three categories:

- Path loss: it is the attenuation experienced by radio waves as they propagate through space.
- Large-scale fading (shadowing): causes variations over larger areas, and is caused by terrain, building, and foliage obstructions.
- Small-scale fading: variations of instantaneous signal strength over very short time intervals or very short distances with respect to the wave length.

Usually, the strong variations experienced in the channel have a direct impact on the performance of radio links, since they require a minimum received signal strength, or Signal-to-Noise Ratio (SNR) to maintain the communication. In order to estimate the signal attenuation between the transmitter and receiver, a proper radio channel model must be used in the design of wireless systems. In the context of wireless communications, a wireless channel model is a mathematical representation of radio wave propagation as a function of frequency, distance and other conditions present in the environment. It is worth remembering that different frequency bands have different propagation characteristics, meaning that a channel model for a specific frequency band could not be accurate for other frequency bands. As a result of these characteristics, different models exist for different types of radio links under different conditions.

Wireless channel models can be divided into three main groups [57]:

- Empirical models: are based on extensive observations and measurements. These models predict mean path loss as a function of various parameters, for example, distance, antenna heights, etc.
- Deterministic models: determine the received signal power at a particular location by using propagation characteristics of radio waves. Geometric and electromagnetic characteristics are easily stored digitally, and computer simulation are used for the propagation. Some estimation methods allow the impact of different propagation mechanisms to be independent of each other. However, a disadvantage is the large amount of calculations, i.e., the heavy computational burden, needed during data preprocessing and simulations.
- Stochastic methods: model the channel as a series of random variables. These models are the least accurate but require the least information about the environment and use much less processing power to generate predictions. Instead of trying to determine the field strength or received power in each point of the coverage area, stochastic models determine the probability density function of a wide range of the field strength information.

As mentioned before, due to the particularities of radio propagation in indoor, a RT-based propagation tool has been selected in this study. Brief descriptions of both empirical and deterministic models are presented next for the sake of completeness. Interested readers are refereed to [18], [58] for an in-depth treatment of stochastic methods

**Empirical models**

Empirical channel models can be used to represent indoor and urban environments, and they have been used thoroughly in the history of wireless systems. Some of the most relevant empirical models are:

- Okumura-Hata model: In 1968, Okumura conducted extensive measurements of base station to mobile signal attenuation in Tokyo's urban environment, and developed a set of curves giving median attenuation relative to free space path loss. Later in 1980, Hata developed mathematics expressions for Okumura's curves. Okumura-Hata model is intended for distances greater than 1 km, making it ideal for macro cells. The antenna height is also assumed to be higher than the surrounding rooftops. It is also designed for frequencies between $150 - 1500$ MHz. this characteristics make the model ideal for the first and second generation of mobile networks. The equation for the average path loss is:

$$L = 69.55 + 26.16\log_{10}(f) - 13.82\log_{10}(h_{\mathrm{t}}) \\ - a(h_{\mathrm{r}}) + (44.9 - 6.55\log_{10}(h_{\mathrm{t}}))\log_{10}(d) \quad [\mathrm{dB}].$$

  where $f$ is the carrier frequency, $h_{\mathrm{t}}$ is the transmitter antenna height and can range from 30 to 200 meters, $h_{\mathrm{r}}$ is the receiver antenna height and can range from 1 to 10 m, $d$ is the distance in kilometers between transmitter and receiver and can range from 1 to 10 km, and $a(h_r)$ is a correction factor depending if it is a small and medium city or a large city. Further information can be found in [58].

- COST 321: The European Cooperative for Scientific and Technical (COST) extended the Okumura-Hata model from 500 MHz to 2000 MHz. It also contains corrections for urban, suburban and rural environments.The basic equation for median path loss in dB is:

$$L = 46.3 + 33.9\log_{10}(f) - 13.82\log_{10}(h_{\mathrm{i}}) \\ - a(h_{\mathrm{r}}) + (44.9 - 6.55\log_{10}(h_{\mathrm{t}}))\log_{10}(d) + C_{\mathrm{m}} \quad [\mathrm{dB}].$$

  where $f$ is the carrier frequency, $h_{\mathrm{t}}$ , $h_{\mathrm{r}}$ , and $a(h_{\mathrm{r}})$ can have the same values as Hata model, $d$ is the distance between transmitter and receiver and can range from 1 to 20 km, $C_{\mathrm{m}}$ is 0 dB for medium cites and suburban areas and 3 dB for metropolitan areas. Further information can be found in [58].

- ITU-R M.2135: Channel models included in the guidelines for the evaluation of radio interface technologies for IMT-Advanced. The channel models are specified in the frequency range from 2 GHz to 6 GHz and for different antenna heights. For rural macro cell scenario, the channel model can be used for frequencies down to 450 MHz. The channel model involves a series of path loss equation depending on different scenarios, the equation for the indoor scenario with line of sight is:

$$PL = 16.9\log_{10}(d) + 32.8 + 20\log_{10}(f_{\mathrm{c}}) \quad [\mathrm{dB}].$$

where $f_c$ is the carrier frequency, $d$ is the link distance between 3 and 100 m, the antenna height for the transmitter must be from 3 to 6 m and the antenna of the receiver from 1 to 2.5 m. The complete set of channel equation for different scenarios and layouts is found in [59].

It is worth remembering that these models are made by collected statistical measurements. Therefore, they can represent broadly the different scenarios where they might be used. If the studied environment doesn't have similar characteristics, the resulting median path loss can be over or underestimated. This is essentially the reason why these models cannot be applied to accurately characterize the propagation in indoor environments.

### Deterministic models

Unlike empiric models, deterministic models are physically meaningful and potentially accurate. Their drawback is that they can only represent the specific studied environment, making them useful in a case-by-case fashion. Another disadvantage is the heavy computational processing that is required,, hence data preprocessing and simplification work must be done in advanced. They also require precise databases, including the location geometry of obstacles and electromagnetic parameters of the materials. The most common methods are optical models called ray launching or ray tracing, and Finite Difference Time Domain based on Maxwell's equations [57].

- Ray tracing: This method uses the principles of optics to simulate the propagation of electromagnetic waves, particularly ray reflection calculation. It works by calculating image sources of the original transmitter on surrounding surfaces, and pointing towards the receiver. In general, only the closest surfaces are considered as secondary images of the transmitter, but the number of reflections and diffractions is usually set prior to simulations.

  The interactions between objects are tracked with a tree structure called visibility tree. At the root of the tree is the transmitter, and the nodes in the first layer correspond to all objects with a direct path to the transmitter. Each node of the tree represents an object that interacts with the rays, and each branch represents a line of sight connection between two nodes. The construction of the tree continues until it reaches the maximum amount of specified layers [60]. Software tools are used for the creation of the visibility tree in the stage known as preprocessing. After this stage is completed, the prediction is reduced to a search in a tree structure.

  In this thesis, the method Intelligent Ray Tracing used in ProMan is used. In Intelligent Ray Tracing, the walls and edges of the 3D model are divided into segments and further divided into tiles. The visibility tree is then created using the centres of the segments and tiles as the tree's objects. The tiles, segments and visibility tree of Proman can be seen in Figure 13.

- Ray launching: also known to as Shooting and Bouncing Rays, is a different ray optics based method. This technique launches a great number of rays from

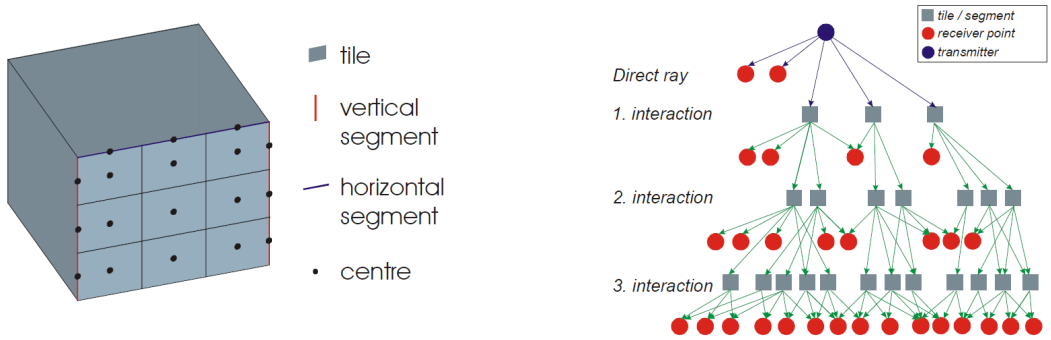


(a) Tiles and segments. (b) Visibility tree.

Figure 13: Intelligent Ray Tracing method.

the transmitter. The paths are determined by looking for the rays that end on the receiver. The transmitter and the receiver are represented as discrete point in a three dimensional environment, hence it is important to consider the rays' angle in order to find all the possible paths.

- Finite Difference Time Domain (FDTD): deterministic methods that solves Maxwell's equations. They can accurately calculate the parameter values of a spatial point and explain the effects of reflection, diffraction and radiation. FDTD provide the information for every point in the desired area while also giving information of the whole region [57]. The drawback for its accuracy is the extensive storage and computations the method requires. For this reason, FDTD has been used to verify other modeling techniques and to study near field problems around the antennas [60].

As it has been explained, deterministic channel models mentioned can be really accurate, and are widely used in indoor environments modeling. With the reasoning, and taking advantage of the existing 3D model for the building, Intelligent Ray Tracing tools were adopted in this thesis.

## 3.2 Multiobjective optimization and NSGA-II

This section explains the third stage of the framework as indicated in Figure 11, which aims at topology optimization. Network optimization is usually the last step performed when deploying a mobile network, however, optimization is also attractive before initial deployment of indoor mobile networks, as a careful planning can substantially improve system performance. Thus, in order to address this task, this thesis uses multiobjective optimization, specifically multiobjective evolutionary algorithms. This section gives an overview of both topics, while the mathematical formulations are explained in section 4.2.

Real life scenarios usually involve different objectives to optimize that can be conflicting in nature, where optimizing one objective implies worsening the others. For example, a production line must minimize cost while maximizing performance, and a

mobile network must minimize interference while maximizing coverage, or maximize capacity while minimizing interference. Multiobjective optimization (MO) [61] is the discipline that studies the resolution of problems involving more than one *objective* function. Since a single optimal solution of a multiobjective optimization that maximizes each objective function is almost impossible, a set of solutions comprises the solution of these type of problems. As a set, these solutions represent the best possible tradeoff among the objective functions. This set is known as Pareto Front (PF) [62], and it offers a wide and complete view of the context-and-problem-specific tradeoffs.

Given an optimization scenario with $K$ objectives, where there is no clear preference of one objective over another, a minimization multiobjective problem for $K$ objectives involves an $n$-dimensional decision vector (there are $n$ design variables) $x = x_1, x_2, ..., x_n$ s.t. $x \in X$ where X is the solution space. We must find a vector $x^*$ that minimizes a set of $K$ objective functions $z(x^*) = z_1(x^*), z_1(x^*), ..., z_n(x^*)$. The solution space $X$ usually has a series of constraints such as $g_j(x^*) = b_j$ for $j = 1, ...m$ and decision function bounds.

Suppose two different feasible solutions $x_1$ and $x_2$ are presented. The solution $x_1$ dominates $x_2$ ($x_1 \succ x_2$) if and only if $z_i(x_1) \leq z_i(x_2)$ for $i = 1, ..., K$, meaning that $x_1$ is better than $x_2$ in at least one objective function $j$ ($z_j(x_1) < z_j(x_2)$), and it is not worse in the others. If a solution is not dominated by any other solution, it is said to be a Pareto optimal solution [63].

The goal of multiobjective optimization is to find the set of solutions which are not dominated by any other solution, usually called the Pareto optimal set, whose corresponding function values are referred as Pareto Front. However, when solving a multiobjective optimization problem, it may be impossible or complex to find the Pareto Optimal set due to its size. Therefore, methods are needed to approach the optimal set while maintaining a reasonable complexity. This Pareto set approximation must comply with three different goals: it should be as close as possible to the Pareto optimal set, ideally a subset; the solutions in the approximation should be evenly distributed among the Pareto optimal set; and the approximation should cover all the spectrum of the Pareto optimal set. To determine if the set is a good approximation, the hypervolume metric is the most used method nowadays. This metric measure the hypervolume of the space dominates by the images of the solutions and a reference point [64].

From the many multiobjective optimization algorithms available, Multiobjective Evolutionary Algorithms (MOEA) are comprehensively used in real life problems because they do not require prioritization, scale or weighted objectives. MOEAs are able to simultaneously search and find different solutions in problems with non-convex, discontinuous and multi-modal solution spaces [65].

In general terms, MOEAs are Genetic Algorithms (GA), a subset of evolutionary algorithms, a population based search techniques inspired on the evolution theory of the origin of species. In the Darwinist theory, organisms that weak and unfit to their environment will face extinction while, the best adapted organism continues to reproduce. Eventually, the better suited organisms become dominant in the environment. Additionally, mutations will occur during the evolutionary process,

and new species will appear if the mutations are beneficial.

Evolutionary algorithms have the following elements:

- chromosome: also known as individuals, are data structures that correspond to a unique solution vector in the solution space. They are composed of units called genes that determine the features of the chromosome.
- population: a collection of chromosomes. At the beginning of the algorithm it is usually randomly generated and will eventually converge to a single solution.
- mating selection: method that determines which and how the chromosomes are selected to generate new chromosomes. In general, fitness is directly related to the probability of reproducing. Different algorithm use different selections like proportional selection, ranking, and tournament selection.
- environmental selection: chooses which individuals should remain in the population for the next generation. mating and generations are the most basic form of environmental selection. Elitism is also a popular method, where the best individuals always remain in the population. Elitism guarantees that the solution obtained by the algorithm will not decrease in future generations.

GA use two different kinds of operators to generate new individuals:

- crossover: operator that combines the traits of two chromosomes in order to create a new one, called *offspring*.
- mutation: operator that will randomly change the genetic traits of an individual as a mean of keeping diversity.

Crossover is the most important operator of both. The chromosomes are combined through the methods established in the mating selection, which prefer fitness. The resulting offspring will then inherit genes that result in better fitness. As more generations are created, these genes will appear more frequently in the population, converging to a good solution. On the other hand, mutation is introduced to change the traits of genes in chromosomes. The probability of mutation in a gene is low and depends on the length of the genes. The introduction of mutations is important to avoid a situation where the population is mostly identical, essentially broadening the search space and avoiding local optima [63].

Out of the different MOEAs available, NSGA-II was selected for its characteristics. NSGA-II is a well-known MOEA [66], whose main characteristics are: its parameterless approach and efficient constraint-handling method through the use of elitism and fast non dominated sorting procedure.

The population is divided into non dominated fronts, and when the current and next generations are merged, the best individuals remain in the next generation. NSGA-II introduces a term called *crowding* distance, where each individual is assigned a value that is equal to the sum of the distances to the nearest neighbors. Best solutions have a crowding distance set to infinity.

NSGA-II doesn't explicitly compute a fitness function, instead, when comparing two individuals, it compares the number the non dominated front the individuals belong to, the individual with the lower number is selected as a winner. If both individuals belong to the same non dominated front, crowding distance is used as a tiebreaker, and the individual with the larger crowding distance is selected. An direct advantage of elitism and the non dominated sorting is a better spread of solutions and better convergence near the true Pareto optimal front compared to other elitist MOEAs. However, NSGA-II works better with two or three objectives, after that the dominance relation is practically nonexistent [64]. The full algorithm of NSGA-II is as follows:

1. Initial population $P_0$ of size $N$ is created at $t = 0$.
2. Crossover and mutation are applied to $P_0$ to create an offspring population $Q_0$ of size $N$.
3. Combine the two populations $R_t = P_t \cup Q_t$.
4. Apply non dominated sorting algorithm to $R_t$ to find the non dominated fronts $F_1, F_2, \ldots, F_k$.
5. Calculate crowding distances of every $F_i$ solution for all $k$ non dominated fronts.
6. Create a new population $P_{t+1}$ of size $N$. If $|P_{t+1} + |F_i| \leq N$, then $P_{t+1} = P_{t+1} \cup F_i$. Else if $|P_{t+1} + |F_i| > N$, then add the least crowded $N - |Pt + 1|$ solutions from $F_i$ to $P_{t+1}$.
7. Use crowding distance to select parents from $P_{t+1}$. Crossover and mutation are used to create offspring population $Q_{t+1}$ of size N.
8. Finally, increase simulation time $t = t + 1$.

To stop the algorithm, there is usually a termination criteria or a maximum number of generations.

The objectives and formulations necessary for NSGA-II optimization in the indoor scenario are presented in section 4.2. After NSGA-II has finished, an evaluation of the topologies is needed to determine if the system model or any performance metric needs adjustments. This assessment is performed by the system-level simulator.

## 3.3 System-level simulations

This section describes the fourth step (see Figure 11) in the proposed framework, System-level simulations. It gives an overview of SLS and their importance for performance evaluation of the network topologies.

In this study, system-level simulations are need to validate the performance of the optimized topologies. SLS also serve as a tool to fine-tune the system model if the behavior of one performance indicator does not match at system-level.

### 3.3.1 Link-level and system-level simulations

In a mobile systems context, simulations are used extensively to test and optimize equipment, algorithms and other procedures where abstractions and simplifications are made in order to research topics that are too complex to be studied analytically [67].

In LTE, as a very complex system, extensive use of simulations during all stages of development are required. Generally, simulations in wireless systems can be categorized as link-level simulations (physical layer) and system-level simulations (network layer) [68].

Link-level simulations are used to evaluate the performance of the physical layer, radio access, radio interface, and transmission related methods. A distinctive characteristic of link-level simulation is that it focuses in one continuous radio link, it can then focus on channel modeling, modulation, synchronization, multi antenna techniques etc.

On the other hand, system-level simulations are focused on evaluating the performance of the network with metrics such as system throughput, scheduling, mobility, interference management, etc. System-level simulations model the various eNodeBs and UE in the network. Simulating all the elements of the network would at a physical layer would take extensive computation and resources, so it is best to use simplified abstractions and obtain the relevant information from them. The abstraction of the physical layer can be obtained from link-level simulations and used by system-level simulators via a mapping called link-to-system (L2S) mapping [67], [68]. L2S mapping data normally includes SINR or Block Error Rate (BLER), that can easily be used to compute network metrics.

An important point to remember is the variability of SLS. SLS is susceptible principally to the scheduler used, as schedulers may have different goals such as maximizing system throughput, maximizing throughput of weakest cell, maintaining fairness among users, capacity based on data pricing, etc. Other factors affecting the system throughput are scheduler specific parameters, retransmission techniques, multi antenna techniques. Hence, SLS configurations require thoughtful decision to be in compliance with the system that is intended to be studied and evaluated.

### 3.3.2 Structure and overview of the simulator

This section describes on a high level the system-level simulator created for this thesis, the inputs, modules, and outputs.

The system-level simulator used in this thesis is MATLAB-based, and allows us to evaluate each topology on under more realistic assumptions, such as QoS-oriented scheduling, link adaptation, and so on. The blocks diagram can be seen in Figure 14.

The simulator has two main input blocks:

- propagation simulation results of the indoor environment for every candidate location $L_L$.
- multiobjective optimization results, i.e., the set of optimized network topologies that are required to be analyzed at system level.

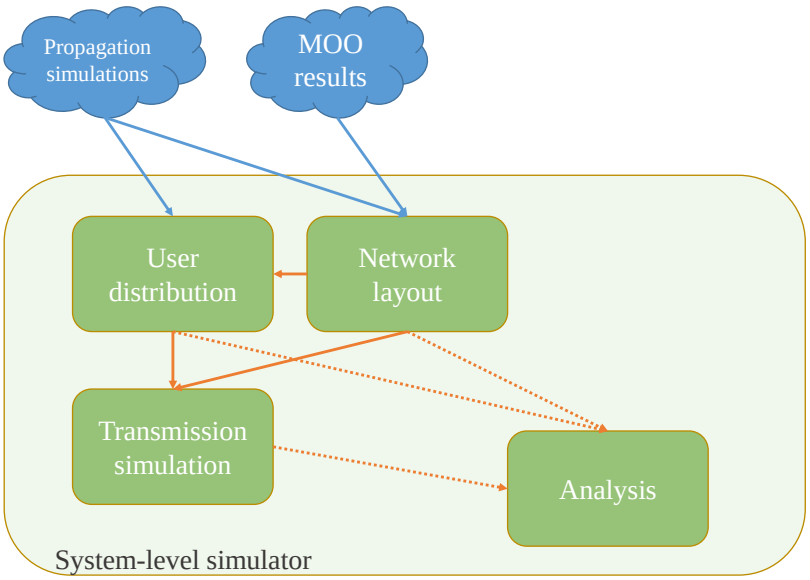


Figure 14: System-level simulator functioning blocks.

Internally, the simulator can described with four different blocks:

- Network layout: this block takes the information generated from the multiobjective optimization and the propagation simulations of the candidates locations. It will then construct the network layout according to the Pareto efficient topologies using the propagation data. The network has information in every pixel, such as received signal strength and SINR, as well as physical parameters of the whole network area such as, system bandwidth, carrier frequency, coverage, received signals strength and SINR maps.

- User distribution: this block generates the users of the network and allocates them inside the desired indoor area accordingly to a spatial distribution. The users are allocated to the corresponding node, are assigned them a network service (a particular type of traffic), and receive the SINR value corresponding to the pixel in which they were generated. For this simulator, no user mobility is considered, i.e., users are static throughout the simulation time, but each independent simulation last for a period of time long enough to capture the nature of each type of traffic and let the scheduler to converge a *stable* performance state. Link-to-system mapping is done at this stage, where SINR computed at the user distribution block is mapped into Channel Quality Indicator (CQI) values using Shannon's capacity theorem and the 4-bit CQI table 7.2.3-1 found in [69] and presented as Table 6.

- Transmission simulation: this module performs downlink transmissions for all nodes and for every user inside the coverage area. The actions involved in include realistic traffic patterns, data buffering, and scheduling of resource

blocks. The scheduling used and more data of the specific test case used will be discussed in section 5.1.

- Analysis module: this block functions as an overseeing entity of the simulator, gathering different data and performing the calculations needed to evaluate the network.

Table 6: CQI 4-bit table.

| CQI index | Modulation | Code rate x 1024 | Efficiency |
|---|---|---|---|
| 0 | out of range | | |
| 1 | QPSK | 78 | 0.1523 |
| 2 | QPSK | 120 | 0.2344 |
| 3 | QPSK | 193 | 0.3770 |
| 4 | QPSK | 308 | 0.6016 |
| 5 | QPSK | 449 | 0.8770 |
| 6 | QPSK | 602 | 1.1758 |
| 7 | 16QAM | 378 | 1.4766 |
| 8 | 16QAM | 490 | 1.9141 |
| 9 | 16QAM | 616 | 2.4063 |
| 10 | 64QAM | 466 | 2.7305 |
| 11 | 64QAM | 567 | 3.3223 |
| 12 | 64QAM | 666 | 3.9023 |
| 13 | 64QAM | 772 | 4.5234 |
| 14 | 64QAM | 873 | 5.1152 |
| 15 | 64QAM | 948 | 5.5547 |

Due to the statistical nature of the system model and the spatial service demand distribution used in this thesis, system-level simulations have to follow a Monte Carlo method for them to be statistically significant. This will make sure that the simulations are representative of the whole network and not dependant in a single simulation specific parameters. It is also important to simulate different service loads in the network in order to estimate the service demand that can be supported by each network topology.

## 3.4 Remarks

The proposed framework functionalities and its modules, apart from the system model and the optimization problem formulation, were explained in this chapter. The framework focus is aimed at indoor planning based on a statistical system model as a complementary tool in the current research of LTE-U. In addition, an overview of wireless channel modeling and multiobjective optimization was provided. Conclusions of this chapter can be summarized as follows:

- Indoor environments need precise models to represent them, making the modeling of indoor environments challenging and in many times case-specific. Accurate 3D models and materials databases are a popular tools that allow to model the layout of indoor environment, as well as material characteristics relevant to radio waves propagation.
- Deterministic models accurately describe the radio propagation. In addition, when 3D model is presented, ray tracing (RT) is the preferred prediction technique.
- When deploying a new indoor mobile network, the spatial placement of the nodes is crucial to maximize the benefit from the network and radio resources as well as enhance users experience. This is very important as networks start to densify because dense networks imply larger interference, which is the main capacity-limiting factor in many wireless systems.
- In order to find the best possible tradeoff, multiobjective optimization has been employed.
- System-level simulations are to be used to evaluate and validate the performance of optimized network topologies under different conditions, such as different service demand volumes, and different services requirements. SLS are also used for fine-tuning the system model when the performance metrics does not match the behavior found at system-level.

# 4 System Model and Network Optimization

This chapter explains the system model and the optimization problem formulation embedded in the framework proposed in Chapter 3. These steps were left for their own chapter to emphasize their importance on the overall work in this thesis.

This chapter is organized as follows: Section 4.1 will explain in detail the system model for the LTE-U network. Section 4.2 presents the optimization problem formulation based on selected performance metrics.

## 4.1 System model

The system model is based on the downlink of an Orthogonal Frequency Division Multiple Access (OFDMA) LTE-U with Frequency Division Duplex (FDD) scheme. As in LTE LAA, the uplink will be assumed to be transmitted over licensed bands, and hence, it is not considered in this model. Along the LTE-U network, a WiFi network using Time Division Multiple Access (TDMA) with Time Division Duplex (TDD) is assumed. Both networks are assumed to use the same channel with bandwidth $B_{\text{ch}}$.

Both networks, LTE-U and WiFi, are deployed in an indoor area, where the indoor coverage area $\mathcal{A}$ is the same for both networks. The WiFi deployment is composed of $L_{\text{W}}$ access points (APs), and the LTE-U network has $L_{\text{L}}$ nodes candidate locations. The coverage area $\mathcal{A}$ can be further divided into small area elements of cardinality $A$ where the received power is constant, therefore, making Signal-to-Interference plus Noise Ratio (SINR) constant. The indexes of the area elements corresponding to the $l^{\text{th}}$ and $i^{\text{th}}$ LTE-U and WiFi AP are $a_{\text{L}}^{l}$ and $a_{\text{W}}^{i}$, respectively.

WiFi APs and candidate locations have omnidirectional antennas and they transmit the same power, i.e., $P_{\text{L}}^{\text{tx}}$ and $P_{\text{W}}^{\text{tx}}$, for LTE-U and WLAN, respectively. The radio propagation, i.e., path loss and antennas gain, is represented by the matrices $\mathbf{G}_{\text{L}} \in \mathbb{R}^{A \times L_{\text{L}}}$ for LTE-U, and $\mathbf{G}_{\text{W}} \in \mathbb{R}^{A \times L_{\text{W}}}$ for WiFi. The vector $\mathbf{x} \in \{1, 0\}^{L_{\text{L}}}$ determines the '*topology*' of the LTE-U network, i.e., if the $l^{\text{th}}$ candidate location has an LTE-U node, then $\mathbf{x}(l) = 1$, and 0 otherwise. since the objective is to determine the best locations for the LTE-U nodes, $\mathbf{x}$ is the optimization variable to achieve the required planning, covered in section 4.2.1.

Cell selection in the LTE-U network is based on average Pilot Symbols (PS) received power, reference symbols in the OFDM time/frequency grid that permit channel estimation. Firstly, the matrix $\mathbf{R}_{\text{PS}} \in \mathbb{R}^{A \times L_{\text{L}}}$, denoting the received power in each area element, is computed as follows:

$$\mathbf{R}_{\text{PS}}\left(\mathbf{x}\right) = \mathbf{G}_{\text{L}} \cdot \text{diag}\left(\mathbf{p}_{\text{PS}} \odot \mathbf{x}\right), \tag{1}$$

where $\mathbf{p}_{\text{PS}} \in \mathbb{R}^{L_{\text{L}}}$ indicates the transmit power in PS (the operators $\odot$ and $\oslash$ indicate Hadamard or pointwise operation for multiplication and division, respectively). The dependence of $\mathbf{R}_{\text{PS}}$ on $\mathbf{x}$ is explicitly indicated. Hereafter, this dependence will be omitted for the sake of clarity. Accordingly, the $a^{\text{th}}$ area element ($a^{\text{th}}$ row in $\mathbf{R}_{\text{PS}}$) will be served by cell $l^{\star}$ if its received power is larger than any other cell:

$$l^{\star} = \underset{l \in \{1,2,\dots,L_{\text{L}}\}}{\text{argmax}} \; \mathbf{R}_{\text{RS}}(a, l). \tag{2}$$

Equations 1 and 2 can be used to built the binary coverage matrices $\mathbf{S}$, and $\mathbf{S}^{\mathrm{c}} \in \{0,1\}^{A \times L_{\mathrm{L}}}$. In this manner, if $\mathbf{S}(a, l^{\star}) = 1$, the $a^{\mathrm{th}}$ area element is served by the node $l^{\star}$. $\mathbf{S}^{\mathrm{c}}$ is the binary complement of $\mathbf{S}$. It is assumed that each area element is only served by one node.

Subsequently, the vector $\mathbf{\Gamma} \in \mathbb{R}^{A}$ contains the SINR value for every area element, and it is given by:

$$\mathbf{\Gamma} = \mathbf{P}^{\mathrm{u}} \oslash \left[ \, \mathbf{I}_{\mathrm{L}} + \mathbf{I}_{\mathrm{W}} + \boldsymbol{\sigma}^{2} \, \right]. \tag{3}$$

where $\mathbf{P}^{\mathrm{u}}$, $\mathbf{I}_{\mathrm{L}}$, $\mathbf{I}_{\mathrm{W}}$, and $\boldsymbol{\sigma}^{2}$ (all $\in \mathbb{R}^{A}$) correspond to the power received from the serving LTE-U node, the interference generated by the LTE-U network, the interference coming from the WiFi network, and the noise power, respectively.

The $a^{\mathrm{th}}$ area element is considered to have LTE-U coverage if that element has SINR and received power values greater than certain thresholds, i.e., $\mathbf{\Gamma}(a) \geq \gamma_{\min}$ and $\mathbf{R}_{\mathrm{PS}}(a, l^{\star}) \geq P_{\min}$ are satisfied. Thus, in order to integrate these coverage criteria and to penalize topologies with coverage gaps, the spectral efficiency of each area element is stored in the vector $\boldsymbol{\eta} \in \mathbb{R}^{A}$ and it is given by

$$\boldsymbol{\eta}(a) = \mathbf{c}(a) \, \cdot \, f_{\mathrm{Link}} \left( \, \mathbf{\Gamma}(a) \, \right), \tag{4}$$

where each element of $\mathbf{c} \in \mathbb{R}^{A}$ is computed as follows:

$$\mathbf{c}(a) = \mathrm{u}\left(\mathbf{\Gamma}(a) - \gamma_{\min}\right) \cdot \mathrm{u}\left(\mathbf{R}_{\mathrm{PS}}\left(a, l^{\star}\right) - P_{\min}\right). \tag{5}$$

The mapping $f_{\mathrm{Link}} : \mathbb{R}_{+} \rightarrow \mathbb{R}_{+}$ [bps/Hz] corresponds to the link performance model and it is usually assumed to be a nondecreasing function of the SINR. In (5), $\mathrm{u}\,(x)$ is the unit step function and it is defined as: $\mathrm{u}\,(x) = 1$ if $x \geq 0$, and 0 otherwise. Recall that $l^{\star}$ is the index of the LTE-U node serving the $a^{\mathrm{th}}$ area element.

In order to built the system model, it is considered that the service demand is known in statistical terms [70], [71]. In the LTE-U network, the service demand is modeled in terms of volume ($M$) and spatial distribution ($\delta_{\mathrm{L}}$). $M$ corresponds to the average number of users in the system, and can be obtained by considering inter-arrival and session times, $\lambda$ and $\mu$, respectively, as random variables. Then, $M = \frac{\mathbb{E}\{\mu\}}{\mathbb{E}\{\lambda\}}$.

The spatial distribution, $\delta_{\mathrm{L}}$, is a Probability Density Function (PDF) that gives the probability of each pixel (area element) $a \in \mathcal{A}$ of having a new user on it. Hence, $\int_{\mathcal{A}} \delta_{\mathrm{L}}(a)\, da = 1$, and consequently $\delta_{\mathrm{L}}(a) \in [0,1]$, $\forall a \in \mathcal{A}$. It is possible to write $\delta_{\mathrm{L}}$ as a vector, and hence, the notation $\boldsymbol{\delta}_{\mathrm{L}} \in \mathbb{R}^{A}$ is also used.

Since WiFi is assumed to be already deployed, traffic statistics are available, i.e., average load ($\alpha \in [0,1]$) and traffic asymmetry ($\rho \in [0,1]$), per access point. For TDD systems, the average load corresponds to the fraction of time with transmissions, either downlink or uplink. The fraction of this *activity* time allocated to downlink transmissions corresponds to $\rho$. Hence, if for a certain period of time, $\alpha_i \triangleq \mathbb{E}\{\alpha_i(t)\} = 0.6$ and $\rho_i = 0.7$, then the $i^{\mathrm{th}}$ WiFi AP and its users use the channel 60% of the time, of which 70% corresponds to downlink transmissions, i.e., the AP is transmitting 42%, receiving 18%, and leaving the channel clear 40% of the time. In order to take into account the uplink interference created by WiFi users, a spatial service demand distribution can be defined. Similarly to LTE-U, a vector $\boldsymbol{\delta}_{\mathrm{W}} \in \mathbb{R}^{A}$

representing the spatial service demand distribution is considered. The notation $\alpha_x$ is used to denote the average load of both LTE-U and WiFi APs[2]. The meaning will be clear from the context, otherwise it will be explicitly indicated. Traffic asymmetry figures only apply to WiFi.

Since LBT is considered, Clear Channel Assessment (CCA) needs to be carried out. Mobile networks are designed to operate under full frequency reuse conditions, with potentially high levels of Intercell Interference (ICI), hence, the CCA is assumed to be based on the interference received from the WiFi network. Thus, the interference received at the $l^{\text{th}}$ LTE-U node, at time $t$, is given by

$$I_l(t) = \sum_{i=1}^{L_{\text{W}}} z_i(t) \left[ I_{i,l}^{\text{d}}(t) + I_{i,l}^{\text{u}}(t) \right]. \tag{6}$$

The $z_i$'s are Bernoulli random variables to model the channel occupancy of the $i^{\text{th}}$ WiFi AP at time $t$. Since its average load is known and given by $\alpha_i$, then $\mathbb{E}\{z_i(t)\} = \alpha_i$. The terms $I_{i,l}^{\text{d}}$ and $I_{i,l}^{\text{u}}$ correspond to downlink and uplink transmissions associated to the $i^{\text{th}}$ WiFi AP. These are given as follows:

$$I_{i,l}^{\text{d}}(t) = P_{\text{W}}^{\text{tx}} \cdot \mathbf{G}_{\text{W}}(a_{\text{L}}^l, i) \cdot \chi_i(t), \tag{7}$$

and

$$I_{i,l}^{\text{u}}(t) = P_{\text{W}}^{\text{tx,u}} \cdot [1 - \chi_i(t)] \cdot \sum_{a \in \mathcal{A}_{\text{W}}^i} \frac{\boldsymbol{\delta}_{\text{W}}(a) \cdot \mathbf{G}_{\text{L}}(a, l)}{\sum_{a' \in \mathcal{A}_{\text{W}}^i} \boldsymbol{\delta}_{\text{W}}(a')}. \tag{8}$$

The $\chi_i$'s are also Bernoulli random variables to model the TDD behavior of WiFi as well as the traffic asymmetry. Hence, $\mathbb{E}\{\chi_i(t)\} = \rho_i$. The random variables $\chi_i$ and $z_i$ are independent. It is considered that the interference generated by WiFi comes either from downlink or uplink. The case of collisions, when both happens at a time, is left for future study as this generalization makes the model significantly more complex (collision probability also depends on load, among other aspects). The average uplink interference received at the $l^{\text{th}}$ LTE-U node, generated from the coverage of the $i^{\text{th}}$ WiFi AP ($\mathcal{A}_{\text{W}}^i$), is obtained by considering the transmit power of WiFi users ($P_{\text{W}}^{\text{tx,u}}$) and their average channel gains, i.e., the sum indicated in (8).

Thus, the probability of an LTE-U node having positive clear channel assessment ($P^{\text{CAA+}}$) is the probability that an LTE-U node receives WiFi interference below a certain threshold, i.e., for the $l^{\text{th}}$ LTE-U node at time $t$

$$P_l^{\text{CAA+}}(t) = \text{P}\left( I_l(t) < I_{\text{CCA}}^{\text{TH}} \right). \tag{9}$$

To complete the system model, we must retake (3), where it can be seen that $\mathbf{P}^{\text{u}} = (\mathbf{S} \odot \mathbf{G}_{\text{L}}) \cdot (\mathbf{p}_{\text{D}} \odot \mathbf{x})$ and $\mathbf{I}_{\text{L}} = (\mathbf{S}^{\text{c}} \odot \mathbf{G}_{\text{L}}) \cdot (\mathbf{p}_{\text{D}} \odot \mathbf{x})$. The vector $\mathbf{p}_{\text{D}} \in \mathbb{R}^{L_{\text{L}}}$ gives the transmission power of each LTE-U node in the data channel. Herein, $\mathbf{p}_{\text{D}}(l) = \mathbf{p}_{\text{PS}}(l) = P_{\text{L}}^{\text{tx}}$, $\forall\, l = \{1, 2, ..., L_{\text{L}}\}$.

Finally, the term $\mathbf{I}_{\text{W}}$ in (3) is required. $\mathbf{I}_{\text{W}}(a)$ corresponds to the average interference received in the $a^{\text{th}} \in \mathcal{A}_{\text{L}}^l$ area element from the WiFi network when obviously

[2]The notion of load in LTE-U APs is similar to WiFi, it refers to the (average) fraction of resources required to satisfy the service demand [72].

$\mathbf{x}(l) = 1$ and the node obtains positive CCA. $\mathcal{A}_{\mathrm{L}}^{l}$ is the set of area elements associated to the $l^{\mathrm{th}}$ LTE-U node. Again, both downlink and uplink components of the interference need to be considered, therefore

$$\mathbf{I}_{\mathrm{W}}(a) = I_{\mathrm{W}}^{\mathrm{d}}(a) + I_{\mathrm{W}}^{\mathrm{u}}(a), \tag{10}$$

where

$$I_{\mathrm{W}}^{\mathrm{d}}(a) = \sum_{i=1}^{L_{\mathrm{W}}} \left[ P_{\mathrm{W}}^{\mathrm{tx}} \cdot \mathbf{G}_{\mathrm{W}}(a,i) \cdot \mathbb{E}\{ z_i \chi_i \,|\, \mathrm{CCA}{+}^{(l^\star)} \} \right], \tag{11}$$

and

$$I_{\mathrm{W}}^{\mathrm{u}}(a) = \sum_{i=1}^{L_{\mathrm{W}}} \sum_{a' \in \mathcal{A}_{\mathrm{W}}^{i}} \left[ P_{\mathrm{W}}^{\mathrm{tx,u}} \cdot \frac{\boldsymbol{\delta}_{\mathrm{W}}(a') \cdot \mathbf{G}(a',a)}{\sum_{a'' \in \mathcal{A}_{\mathrm{W}}^{i}} \boldsymbol{\delta}_{\mathrm{W}}(a'')} \cdot \mathbb{E}\{ z_i \, (1 - \chi_i) \,|\, \mathrm{CCA}{+}^{(l^\star)} \} \right]. \tag{12}$$

In (11) and (12), $\mathrm{CCA}{+}^{(l^\star)}$ indicates the event that the LTE-U node $l^\star$ (the one serving the $a^{\mathrm{th}}$ area element) obtains positive CCA. The matrix $\mathbf{G} \in \mathbb{R}^{A \times A}$ contains the full network geometry, i.e., the average channel gain of each pixel with respect to each other. Note that, indeed, $\mathbf{G}_{\mathrm{L}}$ and $\mathbf{G}_{\mathrm{W}}$ are submatrices of $\mathbf{G}$. These submatrices are generated *offline* using measurements or simulations, but it is worth noting that $\mathbf{G}$ is sparse due to the high isolation of indoor environments. Hence, memory requirements are much less than $A \times A$.

In general, evaluating (9) and the conditional expectations[3] [73] in (11) and (12) is difficult, and only under very restrictive assumptions, closed forms exists. However, as these figures depends on the service demand and network geometry (both known), they only need to be numerically evaluated once and *a priori*. In this thesis, the focus is placed on the important particular case of highly asymmetric traffic: the case when it can be assumed that the WiFi interference is only generated by the APs, i.e., downlink. Under this assumption, the model gets significantly simplified. Thus, if $\rho_i = 1, \ \forall\, i = 1, 2, \cdots, L_{\mathrm{W}}$, then $I_l(t)$, see (6), becomes

$$I_l(t) = \sum_{i=1}^{L_{\mathrm{W}}} z_i(t) \cdot I_{i,l}^{\mathrm{d}}(t) = z_i(t) \cdot P_{\mathrm{W}}^{\mathrm{tx}} \cdot \mathbf{G}_{\mathrm{W}}(a_{\mathrm{L}}^{l}, i). \tag{13}$$

Similarly,

$$\mathbf{I}_{\mathrm{W}}(a) = \sum_{i=1}^{L_{\mathrm{W}}} \left[ P_{\mathrm{W}}^{\mathrm{tx}} \cdot \mathbf{G}_{\mathrm{W}}(a,i) \cdot \mathbb{E}\{ z_i \,|\, \mathrm{CCA}{+}^{(l^\star)} \} \right]. \tag{14}$$

Therefore, the distribution of $I_l(t)$ is required. Equation (13) represents a weighted sum of Bernoulli random variables that can be approximated as a Gaussian random variable when $L_{\mathrm{W}}$ is large. Unfortunately, this is not always the case, but in such cases the numerical estimation of the distribution is very simple. Figure 15 shows the Gaussian Root Mean Square (RMS) error approximation as a function of the number of interferers ($L_{\mathrm{W}}$) for different ranges of the weights, i.e., the constants $P_{\mathrm{W}}^{\mathrm{tx}} \cdot \mathbf{G}_{\mathrm{W}}(a_{\mathrm{L}}^{l}, i)$ in (13). These weights represent the difference in the received power from the WiFi APs. As a reference, an RMS of 2% (which can be considered an

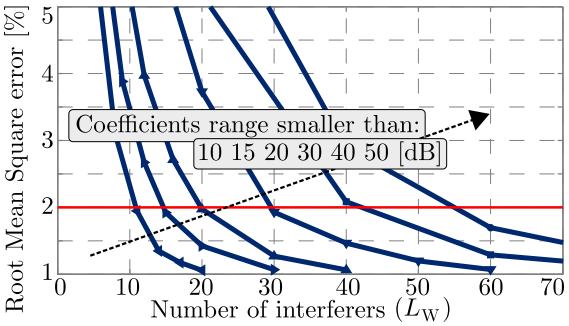


Figure 15: Gaussian approximation: weighted sum of Bernoulli distributed independent random variables.

acceptable approximation in this context) is indicated in red. Finally, regarding (14), it is easy to see that

$$\begin{aligned}\mathbb{E}\{\, z_i \,|\, I_l(t) < I_{\mathrm{CCA}}^{\mathrm{TH}} \,\} &= P\left(z_i = 1 \,|\, I_l(t) < I_{\mathrm{CCA}}^{\mathrm{TH}}\right) \\ &= \frac{P\left(z_i = 1\,;\, I_l(t) < I_{\mathrm{CCA}}^{\mathrm{TH}}\right)}{P\left(\, I_l(t) < I_{\mathrm{CCA}}^{\mathrm{TH}} \,\right)} \\ = \frac{P\left(\sum\limits_{j=1;j\neq i}^{L_{\mathrm{W}}} P_{\mathrm{W}}^{\mathrm{tx}} \cdot \mathbf{G}_{\mathrm{W}}(a_{\mathrm{L}}^l, j) < \left[I_{\mathrm{CCA}}^{\mathrm{TH}} - P_{\mathrm{W}}^{\mathrm{tx}} \cdot \mathbf{G}_{\mathrm{W}}(a_{\mathrm{L}}^l, i)\right]\right)}{P\left(\, I_l(t) < I_{\mathrm{CCA}}^{\mathrm{TH}} \,\right)}&,\end{aligned} \tag{15}$$

which can easily be evaluated for small values of $L_{\mathrm{W}}$.

## 4.2 Indoor planing optimization

The objective of this phase of the framework is to assess the possible LTE-U topologies, subject to WiFi operation and fair coexistence requirement. The output of this phase will be a set of Pareto efficient topologies that can be used for optimal indoor planning. Apart from improving conventional methods for indoor planning that rely on empirical and intuitive methods, optimization are a necessary too to asses the number of topologies, as the possible number of network topologies increase exponentially ($2^{L_L}$) with a larger number of candidate locations.

### 4.2.1 Multiobjective optimization formulation

Herein, the interest is on maximizing the aggregate capacity of the LTE-U network for a given number of nodes, subject to the presence of WiFi and a minimum required coverage. Thus, bearing in mind the previously introduced system model, the following two objective functions are defined:

$$f_1(\mathbf{x}) = \mathbf{x} \cdot \mathbf{1}, \tag{16}$$

[3]The conditional expectation of the random variable $X$ given the event $B$ is defined as follows: $\mathbb{E}\{X|B\} \triangleq \sum_x x\, f(x|B)$, being $f(x|B)$ the conditional density of $X$ given $B$.

that corresponds to the number of LTE-U APs in a certain topology $\mathbf{x}$, and

$$f_2(\mathbf{x}) = (B_{\text{ch}} \cdot A) \left[ \left[ (\boldsymbol{\eta} \odot \boldsymbol{\delta}_{\text{L}})^{\text{T}} \cdot \mathbf{S} \right] \odot \mathbf{n} \odot \mathbf{P}^{\text{CAA+}} \right] \cdot \mathbf{1}, \tag{17}$$

that corresponds to the sum of average capacity of the LTE-U nodes; the dependence on $\mathbf{x}$ is implicit in (17) as $\boldsymbol{\eta}$ and $\mathbf{S}$ depend on $\mathbf{x}$, see (2) and (5). The vector $\mathbf{n} \in \mathbb{R}^{L_{\text{L}}}$ indicates the inverse of the number of area elements served/associated to each LTE-U node. It is adopted by convention that if $\mathbf{x}(l) = 0$, then $\mathbf{n}(l) = 1$ because in such case, the $l^{\text{th}}$ element of the vector $(\boldsymbol{\eta} \odot \boldsymbol{\delta}_{\text{L}})^{\text{T}} \cdot \mathbf{S}$, that represents the average capacity of each AP, is also zero. The joint use of $\boldsymbol{\delta}_{\text{L}}$ and $A$ in (17) captures the impact of the spatial distribution of the service demand on the resulting average capacity, by weighting more the area elements where traffic is more likely to appear. The use of $\mathbf{P}^{\text{CAA+}} \in \mathbb{R}^{L_{\text{L}}}$ scales the achievable rate of each AP by its probability of having positive CCA. Thus, $\mathbf{P}^{\text{CAA+}}$ is created directly by evaluating (9) for each $l$, independently of the value of $\mathbf{x}(l)$. This only needs to be done once because $\mathbf{P}_l^{\text{CAA+}}$ only depends on the WiFi network load (the $\alpha_i$'s) and network geometry. All together, $f_2$ represents the aggregate capacity of the LTE-U deployment specified by $\mathbf{x}$ and its unit is bps as it is considered that the whole channel bandwidth $B_{\text{ch}}$ is reused in each LTE-U AP, so full reuse is assumed.

Thus, proposed multiobjective optimization problem can be written as follows:

$$\underset{\mathbf{x}}{\text{minimize}} \quad \mathbf{f} = [\ f_1(\mathbf{x}),\ -f_2(\mathbf{x})\ ], \tag{18a}$$

subject to:

$$O_{\max} \geq 100 \cdot \left(1 - \left[\left(\mathbf{c}^{\text{T}} \cdot \mathbf{1}\right) \cdot A^{-1}\right]\right), \tag{18b}$$

$$\mathbf{x} \in \{0,1\}^L,\ \mathbf{x} \neq \mathbf{0}. \tag{18c}$$

Conditions (18b) y (18c) correspond to the maximum allowed outage ($O_{\max}$) and the *search space* of $\mathbf{x}$, respectively. Problem 18 is NP-complete, and due to the mathematical structure of $f_2$ (with local optima), the use of metaheuristics [62] is proposed. Herein, NSGA-II has been employed. Calibration and some additional guidelines are provided in Section 5.

## 4.3 Remarks

The system model and optimization problem formulation were presented in this chapter apart from the rest of the framework in order to emphasize its importance.

The system model is based on a OFDMA based DL-only LTE-U network sharing the same system bandwidth as a TDMA FDD WiFi network. A general formulation of the interference experienced by the LTE-U nodes was proposed, however, the analysis becomes increasingly difficult when UL and DL is considered. Hence, a highly asymmetric case was studied. The model uses Bernoulli random variables to model the channel occupancy of the different WiFi APs, as long as their average load is known and given. This different statistical approach was chosen as the real scenario is hard to model and such simplification must be made. However, the model

can be further improved if more precise statistical behavior of the WiFi network is known.

Optimization problem formulation was also presented with the respective objective functions. In this thesis, the focus is on maximizing the aggregate capacity of the LTE-U network for a given number of nodes, subject to the presence of WiFi and a minimum required coverage. However, operators should be able to change the objective functions that suit them best. The evaluation of the resulting Pareto efficient topologies is done during SLS, covered in Chapter 5.

# 5 Performance Evaluation

This chapter presents the results obtained by testing a scenario for the proposed framework. Section 5.1 describes the environment selected and the tools and settings used to obtain the propagation simulations, multiobjective optimizations and system-level simulations. Section 5.2 and section 5.3 present the numerical results for the network optimization and system-level simulations respectively. Finally, coexistence between WiFi and LTE-U is analysed from the radio planning perspective based on results.

## 5.1 Test case & parameter settings

The test-case considered for numerical evaluations is the 2$^{\text{nd}}$ floor of the School of Electrical Engineering at Aalto University, Finland, as shown in Figure 17. The building layout, along with the layout of current WiFi APs and the candidate location for LTE-U nodes can be seen in Figure 17.

As described in section 3.1 and section 3.1.1, the 3D indoor model and database were created using the software WallMan, also by AWE Communications, and the radio propagation predictions were performed by the software ProMan using Intelligent Ray Tracing (IRT). The specific setting for IRT followed the recommendations for ProMan, found in [74], and can be seen in Figure 16.

Table 7 includes the rest of the system model settings used for the propagation simulations. An important variable to emphasize is the pixel resolution, or area element $a$ in the system model, used by ProMan to divide the indoor scenario into segments and tiles needed to construct the visibility tree. The pixel resolution is important as it will determine the granularity of the propagation results, so a careful selection is needed. As the pixel resolution is part of the visibility tree, it can not be set in ProMan, but during the preprocessing stage in WallMan.

The matrices $\mathbf{G}_{\text{W}}$, $\mathbf{G}_{\text{L}}$, and $\mathbf{G}$, are constructed by using output text files from ProMan that contain the received power level at each pixel for one node, and combining them. These text files are divided into rows and columns following a matrix representation of the indoor environment.

The user service demand used in the test case follows an irregular spatial distribution, in order to resemble indoor environments more realistically. The distribution is indicated as $\delta_{\text{L}}$ in Figure 17.

Link capacity is derived by Shannon's Capacity theorem, using the mean SINR, $\gamma$, in every pixel and relating it to the CQI table defined in [69], as explained in section 4.1 and section 3.3, respectively.

The system-level simulator uses a full buffer traffic model defined in [75]. The LTE scheduler used is defined in [76], and considers resource sharing among flows of different services, in order to meet their satisfaction levels, a target data rate for this traffic model. The goal of such scheduler is to maintain a sustainable QoS to different flows of differentiated services and requirements, while improving system capacity.

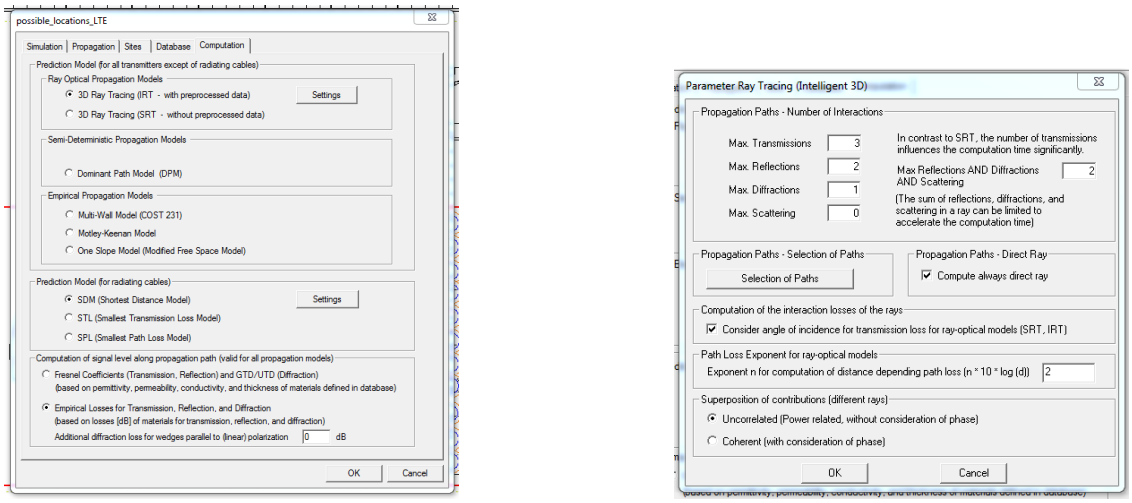


Figure 16: ProMan & Intelligent Ray Tracing settings.

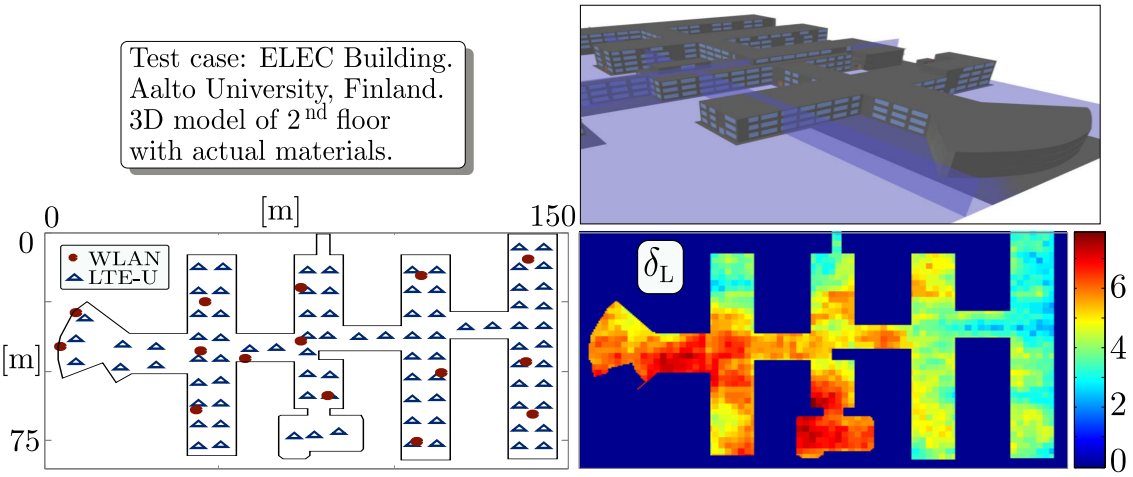


Figure 17: Test case for numerical evaluation.

The rest of the parameters and assumptions, including the calibration of the algorithm NSGA-II [66], are indicated in Table 7.

## 5.2 Multiobjective evolutionary optimization

The solutions of Equation (18) in section 4.2 through multiobjective evolutionary optimization are presented in Figure 18. As indicated in section 4.1, downlink is the only traffic assumed, thus $\rho_i = 1, \forall\, i$. Three different load patterns for WiFi are considered, and shown in Figure 18a:

- *Low* (L) pattern: where $\alpha_i = 0.25, \forall\, i$.
- *High* (H) pattern: where $\alpha_i = 0.75, \forall\, i$.

Table 7: Simulation Parameters and Evaluation Setting.

| | | | |
|---|---|---|---|
| **System model** | | | |
| $L_{\mathrm{L}}$ | 87 | $L_{\mathrm{W}}$ | 15 |
| Area elements | $0.5 \times 0.5\,\mathrm{m}^2$ | $A$ | 20968 |
| Tx. power: $P_{\mathrm{L}}^{\mathrm{tx}}/P_{\mathrm{W}}^{\mathrm{tx}}$ | 15 / 17 dBm | $\sigma^2$ | -174 dBm/Hz |
| SINR min ($\gamma_{\mathrm{min}}$) | -9.4 dB | Sensitivity ($P_{\mathrm{min}}$) | -126 dBm/PS |
| Link: $f_{\mathrm{Link}}(\gamma)$ | $\log_2(1+\gamma)$ | CCA+ ($< I_{\mathrm{CCA}}^{\mathrm{TH}}$) | -94.75 dBm |
| $B_{\mathrm{ch}}$ | 20.0 MHz | $\delta_{\mathrm{L}}$ (see Figure 17) | Non-uniform |
| Antennas | Omni | Antennas gain | 3 dBi |
| Antennas height | 2.4 m | Coverage ($O_{\mathrm{max}}$) | 98% |
| **LTE-based system-level simulations** | | | |
| Resource blocks | 100 | Scheduler | [76] |
| Traffic model | FTP [75] | Target rate $R_{\mathrm{TH}}$ | 1 Mbps |
| Carrier freq. ($f_{\mathrm{c}}$) | 5.8 GHz | Channel feedback | Ideal |
| **Calibration of the algorithm NSGA-II** | | | |
| Population size | 110 | Crossover prob. | 1.00 |
| Type of variables | Discrete | Mutation prob. | $1/L_{\mathrm{L}}$ |
| Termination criterion: *hypervolume* [61] gain $< 0.001\%$ (40 generations). | | | |

- *Intermediate* (I) pattern: where $\alpha_i = [0.1, 0.9]$), i.e., the load of each AP is different.

The resulting Pareto efficient topologies for every WiFi load pattern can be seen in Figure 18b. The advantages of optimization can easily be seen as for all WiFi load patterns, the Pareto fronts show an increase in LTE-U capacity while having a lower amount of nodes ($f_1$ vs. $f_2$). The highest density for patterns L, I, and H is 71, 61 and 61, respectively. These densities translate into a reduced number of nodes in the order of 22% and 29%, and capacity gains of 9%, 10%, and 8% with respect to their respective *all-on* topologies. Conversely, the lowest value of $f_1$ represents the lowest number of nodes needed to provide the coverage seen in Table 7.

Additionally, the statistical model proposed in the system model follows the expected results corresponding to LTE-U nodes following LBT procedure. As LTE-U nodes in different topologies encounter a WiFi network with a higher load pattern, the probability of positive CCA decreases on average.

For a better understanding, a comparison is made between the Pareto efficient topologies of the three different WiFi load patterns (L, I, and H) containing 26 active nodes, $\mathbf{x}_{26}^{\mathrm{L}}$, $\mathbf{x}_{26}^{\mathrm{I}}$, and $\mathbf{x}_{26}^{\mathrm{H}}$, respectively. The networks topologies and respective capacity are shown in Figure 18d, while Figure 18c shows the resulting empirical distribution of successful CCA.

For the topology $\mathbf{x}_{26}^{\mathrm{H}}$, under H load pattern, the mean $P^{\mathrm{CCA+}}$ is 0.51, and its capacity $f_2 = 1.81$ Gbps. The next topology, $\mathbf{x}_{26}^{\mathrm{I}}$, under I load pattern, has a mean $P^{\mathrm{CCA+}}$ of 0.66, and its capacity $f_2 = 1.81$ Gbps; resulting in an increase of 29% in available *air-time*, and an increase of 18% in capacity, with respect to $\mathbf{x}_{26}^{\mathrm{H}}$. The final

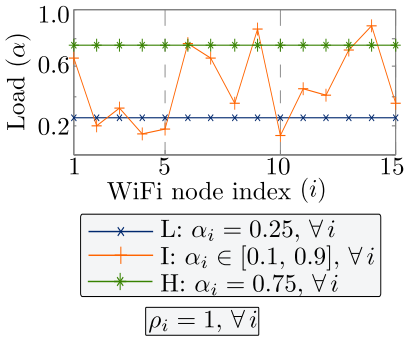


(a) WLAN load patterns.

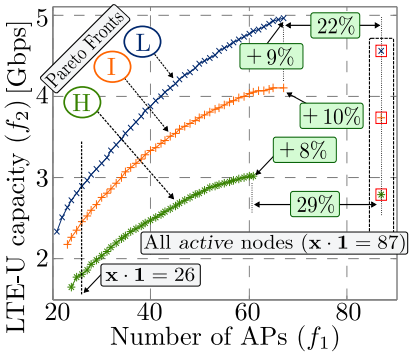


(b) Pareto efficient LTE-U topologies.

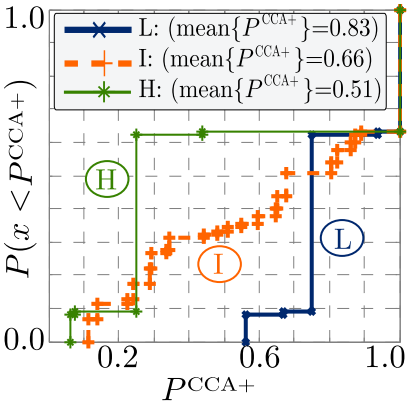


(c) CCA successful probability.

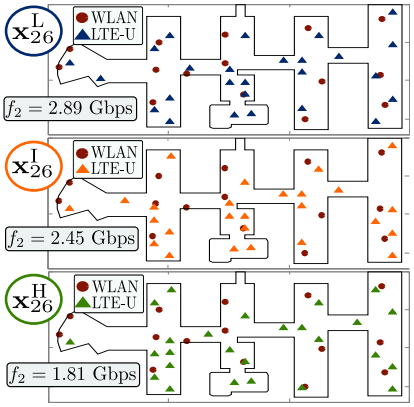


(d) Optimized LTE-U topologies.

Figure 18: Multiobjective optimization for LTE-U indoor planning.

topology, $\mathbf{x}^{\text{L}}_{26}$, under L load pattern, has a mean $P^{\text{CCA+}}$ of 0.83, and its capacity $f_2 = 2.89$ Gbps; resulting in an increase of 35.4% in available *air-time*, and an increase of 60% in capacity, with respect to $\mathbf{x}^{\text{H}}_{26}$.

Hence, the proposed optimization apart from finding the optimal topologies for a WiFi load pattern, it also finds the minimum and maximum density that should be deployed. The minimum density indicates the lowest amount of nodes to meet the coverage requirements, while the maximum number of nodes indicates the threshold when interference becomes the dominating effect in the network instead of frequency reuse. It is worth noting that the highest and lowest number of $f_1$ is highly environment specific. However, the same framework can be applied to any indoor environment about to be deployed or an already existing one with several locations. In addition, other performance metrics can be included, such as, maximizing the throughput of the weakest cell.

## 5.3 System-Level Simulations

As explained in previous chapters, system-level simulations are performed to validate and assess the performance of the toplogies and the framework. The simulation validations follow a Monte-Carlo experiment method, and its results are shown in

Figure 19. The results are based on 500 independent realizations, each of 1000 Transmission Time Intervals (TTIs) of 1 ms, with $M$ users randomly allocated according to the irregular spatial distribution $\delta_{\mathrm{L}}$, seen in Figure 17.

Firstly, the optimality of topologies can be verified by SLS. An example is given in Figures 19c and 19d, where two empiric topologies with $M = 1000$, and minor variation with respect to $\mathbf{x}_{26}^{\mathrm{L}}$ and $\mathbf{x}_{32}^{\mathrm{L}}$, respectively, are compared. Both optimized topologies perform better compared to the empiric ones in terms of users' throughput and and system throughput. For these examples, the small variations amount to a loss of 4% and 5% of system throughput. However, the largest difference in performance can be seen in user throughput, specially on target rate satisfaction, and cell-edge, i.e., users on the lowest $5^{\mathrm{th}}$ percentile.

Within 98% of the target rate satisfaction of 1 Mbps, an acceptable value close to the target rate, the empiric topologies decreased by 7% and 31% for 26 and 32 nodes, respectively. As for cell-edge users, in the 26 nodes empiric topology they were out of coverage, and the 32 nodes topology users on cell-edge throughput decreased by 30%. This behavior can also be seen using the Jain's fairness index [77], see Table 8, a global metric that measures how evenly the resources are shared. Jain's index is bounded on the interval $[1/N, 1]$, where 1 is an equal sharing, and thus best case, and $N$ is the vector containing the capacity measurements of all users. Since all users have the same service in SLS, the ideal outcome of the selected scheduler would be that all users achieve but don't exceed their target data rate. Thus, it can be seen that optimized topologies have a better QoS for all users, compared to the empiric ones.

Other topologies with 26 or 32 APs result in larger losses, and most likely in unacceptable coverage outages. This was extensively verified using SLS. In all SLS, system throughput showed a relatively small difference between empiric and optimized topologies, yet, user experience is greatly affected in empiric topologies. Thus, the optimization for topologies for the specific users distribution can be verified as successful.

Table 8: users satisfaction metrics.

| Topology | Jain's Index | Cell-edge data rate | $P(x < 0.98 * R_{\mathrm{TH}})$ |
|---|---|---|---|
| $\mathbf{x}_{26}$ optimized | 0.9405 | 336 kbps | 0.238 |
| $\mathbf{x}_{26}$ empiric | 0.8945 | 0 bps | 0.2552 |
| $\mathbf{x}_{32}$ optimized | 0.9724 | 500 kbps | 0.13 |
| $\mathbf{x}_{32}$ empiric | 0.9322 | 273 kbps | 0.1887 |

Secondly, validation of dominance relationships among topologies, see Figure 18b, can be verified by SLS. For this purpose, Figure 19a and 19b show a comparison between two topologies in terms of users' rate and system throughput, respectively. Two optimized topologies with 26 and 56 nodes are considered, $\mathbf{x}_{26}^{\mathrm{L}}$ and $\mathbf{x}_{56}^{\mathrm{L}}$, respectively. A service demand volume $M = 650$ that can be handled by $\mathbf{x}_{56}^{\mathrm{L}}$ in a compatible manner with the WiFi load pattern L (see Figure 18a) has been selected to compare $\mathbf{x}_{26}^{\mathrm{L}}$ and

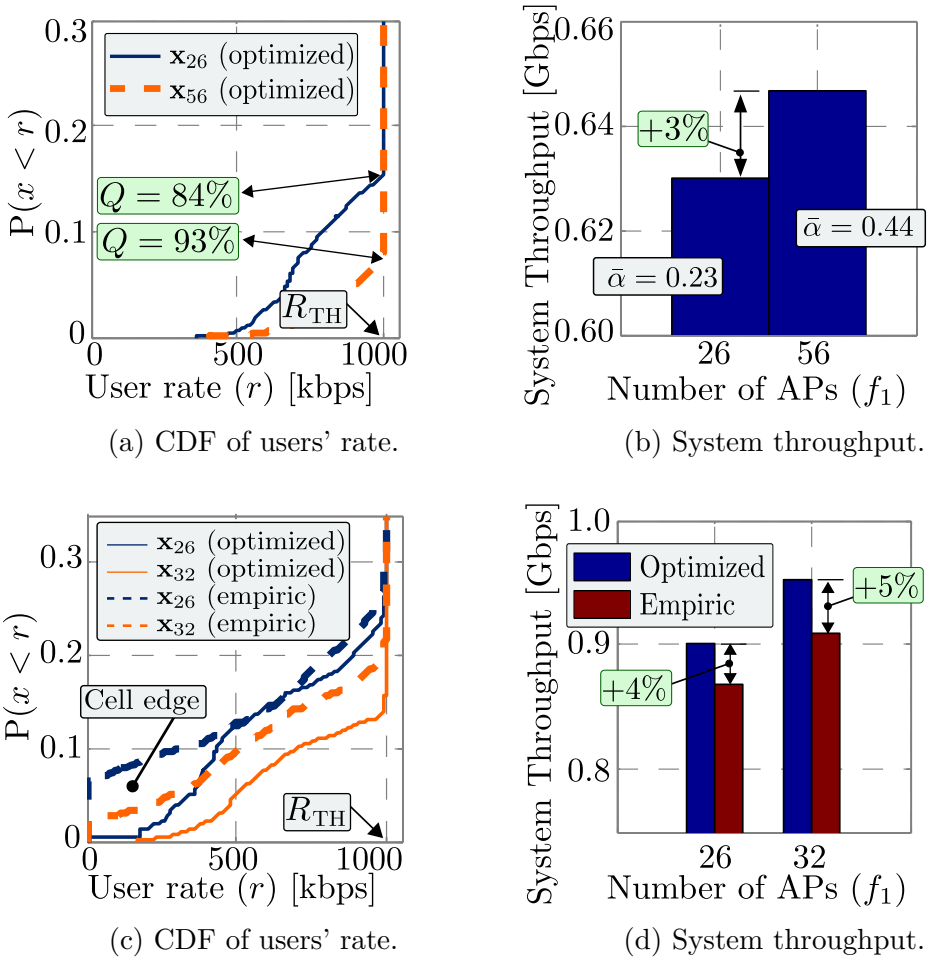


(a) CDF of users' rate.

(b) System throughput.

(c) CDF of users' rate.

(d) System throughput.

Figure 19: Validations: system-level simulations.

$\mathbf{x}_{56}^{\mathrm{L}}$. It can be seen that $\mathbf{x}_{56}^{\mathrm{L}}$ provides a better satisfaction ratio ($Q$) [76], i.e., the percentage of users achieving the target rate $R_{\mathrm{TH}}$, and more importantly, it achieves that while respecting WiFi, i.e., the resulting load of each node is below $P_l^{\mathrm{CAA+}}$. The average load of the LTE-U nodes ($\bar{\alpha}$) is indicated in Figure 19b, where a 3% system throughput improvement is shown. In summary, it is convenient to evaluate the set of Pareto efficient topologies using SLS (for different values of $M$) in order to validate their *system capacity* [76], possibly in terms of other operator-defined service demand volume metrics.

It is important to note that SLS behavior can change depending on the scheduler and network configurations, as well as operator- defined metrics.

Thus, the framework proposed in Figure 11 provides a convenient tradeoff between 1) LTE-U (WiFi friendly) topology optimization (unfeasible using SLS as there are $2^{L_{\mathrm{L}}}$ possible topologies), and 2) finding the demand volumes supported by these topologies under realistic Quality of Service (QoS) and system features (non-tractable mathematically).

## 5.4 Remarks

Optimization results based on the statistical system model were deduced and found to match the behavior seen in reality, i.e., the higher the load in the WiFi network, the achievable capacity for LTE-U is lower.

The results obtained from extensive SLS demonstrate LTE-U topologies coexisting fairly with another system, in this case Wi-Fi, as indicated in the system model, remaining below the $P_l^{\mathrm{CAA}+}$. In addition, different topologies showed different satisfaction levels for users when tested with similar demand volumes, and under realistic QoS requirements using a realistic scheduler.

# 6 Conclusions and Future Work

## 6.1 Conclusions

Operation of LTE in unlicensed spectrum has been recognized as a key feature for current and future development of mobile communications, where indoor traffic will generate the majority of service demand. However, it was shown that the behavior of LTE in the spectrum is not fair and friendly, a major requisite in unlicensed spectrum. Hence, one of the main challenges is to guarantee a fair coexistence between LTE in unlicensed spectrum with other communication systems, specially with WiFi.

Three main research brands of LTE in unlicensed spectrum over the 5 GHz band were reviewed: LTE LAA, LTE-U, and MulteFire. LAA and LTE-U are based in inter-band non-contiguous CA, while MulteFire is planned to be a stand alone deployment. LAA is regarded to be the front runner of the three and it will constitute a global solution following coexistence via LBT. Specifications for LAA and LTE-U are to be released in 2016.

As a complementary tool to the development of LTE in unlicensed spectrum, this thesis focused on network planning and radio access optimization. The contribution consisted in a statistical framework for LTE-U radio access planning and optimization. Once statistically optimized network topologies have been found, performance and validation needs to be performed in SLS, as many real system features cannot be modeled mathematically.

From the optimization and SLS results, conclusions from this study can as follows:

- Accurate 3D models and deterministic models accurately describe the radio propagation. When 3D models are present, ray tracing is the preferred prediction technique.

- As dense networks deployments become common, interference management becomes complex. Thus, careful indoor network planning spatial is valuable to maximize the benefit from the network and radio resources as well as enhance users experience.

- Statistical system models along with multiobjective optimization, provide means to determine the network topologies that maximize the benefit from LTE-U, in a cost-efficient manner. This is necessary in the light of the large number of possible network topologies that are to be compared, which is not feasible by means of SLS.

- Optimized topologies performance found at system level is consistently better in terms of users' rate, QoS requirements, and system throughput. Volume demands supported for such optimized topologies can also be found through SLS. These two results may be directly used for indoor planning or radio access optimization.

- SLS results may differ greatly depending on the accuracy of service demand models and statistics, in particular, load levels, and spatial distribution. These

variables have a profound impact on the resulting inter-system optimization, performance, and coexistence.

- As a novel approach to this problem, several generalizations and refinements need to be investigated. However, the results indicate that those are promising research directions as effective planning is not an alternative but a complementary tool to increase the efficacy of other schemes, such as DCS, LBT, or DC.

## 6.2 Future work

Some recommendations for further study in this topic:

- A case where a non highly asymmetric traffic is assumed in the WiFi network, i.e., a case where UL is included. Such case would be closer to real scenarios, however, the complexity of such scenario is beyond the competence of this study.
- A refined statistical model based on statistical analysis of WiFi networks, as well as optimization based on metrics set by the operator may provide insights closer to real systems.
- Real system experiments where the coexistence and service demand volumes of the proposed framework solutions can be tested and measured.

# References


[1] Ericsson, *Ericsson mobility report, on the pulse of the networked society*, 2014.

[2] Cisco, *Global mobile data traffic forecast update, 2014–2019*, 2015.

[3] R. Wang *et al.*, "Potentials and challenges of c-ran supporting multi-rats toward 5g mobile networks", *Access, IEEE*, vol. 2, pp. 1187–1195, 2014.

[4] R. Zhang *et al.*, "LTE-Unlicensed: The future of spectrum aggregation for cellular networks", *IEEE Wireless Communications*, vol. 22, no. 3, pp. 150–159, Jun. 2015, ISSN: 1536-1284.

[5] B. Coleman *et al.*, *Substantial licensed spectrum deficit (2015-2019): Updating the FCC's mobile data demand projections*, Jun. 2015.

[6] ITU-R, *M. 2074. radio aspects for the terrestrial component of IMT-2000 and systems beyond IMT-2000*, 2005.

[7] Huawei, *Whitepaper on spectrum*, Feb. 2013. [Online]. Available: `www.huawei.com/ilink/en/download/HW_204545`.

[8] 3GPP, "TR 36.889. v1.0.1. 3rd Generation Partnership Project; technical specification group radio access network; study on Licensed-Assisted Access to unlicensed spectrum; (Release 13)", Tech. Rep., Jun. 2015.

[9] 4G Americas, *5G spectrum requirements*, Aug. 2015.

[10] A. Cavalcante *et al.*, "Performance evaluation of LTE and Wi-Fi coexistence in unlicensed bands", in *2013 IEEE 77th Vehicular Technology Conference (VTC Spring)*, IEEE, 2013, pp. 1–6.

[11] N. Jindal *et al.*, "LTE and Wi-Fi in unlicensed spectrum: A coexistence study", Tech. Rep., Mar. 2015.

[12] T. Nihtila *et. al.*, "System performance of LTE and IEEE 802.11 coexisting on a shared frequency band", in *2013 IEEE Wireless Communications and Networking Conference (WCNC)*, IEEE, 2013, pp. 1038–1043.

[13] D. Flore, *3GPP & unlicensed spectrum*, Jan. 2015.

[14] H. Holma *et al.*, *LTE for UMTS: Evolution to LTE-Advanced*. 2011.

[15] 3GPP, *Overview of 3GPP Release 8 V0.3.3 (2014-09)*, Sep. 2014.

[16] 3GPP, *UTRA-UTRAN long term evolution (LTE) and 3GPP system architecture evolution (SAE)*, 2006.

[17] P. Goldstein, *Telia sonera launches first commercial LTE network*, Dec. 2009. [Online]. Available: `http://www.fiercewireless.com/story/teliasonera-launches-first-commercial-lte-network/2009-12-14`.

[18] T. Rappaport, *Wireless communications principles and practice*, ser. written in Chinese. Publishing House of Electronics Industry, 1999, ISBN: 7505348779.

[19] T. Ali-Yahiya, *Understanding LTE and its Performance*. Springer Science & Business Media, 2011.

[20] Telesystem Innovations Inc., *LTE in a nutshell: The physical layer*, 2010.

[21] H. Holma *et al.*, *LTE Advanced: 3GPP solution for IMT-Advanced*. John Wiley & Sons, 2012.

[22] 3GPP, " TR 36.211. v12.8. 3rd Generation Partnership Project; technical specification group radio access network; evolved universal terrestrial radio access (E-UTRA); physical channels and modulation (Release 12)", Tech. Rep., Jun. 2015.

[23] ITU-R, "M.2134. Requirements related to technical performances for IMT Advanced radio interface(s)", Tech. Rep., Nov. 2008.

[24] 3GPP, "TR 36.913. Requirements for further advancements for Evolved Universal Terrestrial Radio Access (E-UTRA)(LTE-Advanced), V8.0.1", Tech. Rep., Mar. 2009.

[25] H. Lee *et al.*, "A survey of radio resource management for spectrum aggregation in LTE-advanced",

[26] 3GPP, "TS 36.300. evolved universal terrestrial radio access (E-UTRA) and evolved universal terrestrial radio access network (E-UTRAN); overall description; stage 2", Tech. Rep., 2012.

[27] A. Checko *et al.*, "Cloud ran for mobile networks—a technology overview", *IEEE Communications Surveys & Tutorials*, vol. 17, no. 1, pp. 405–426, 2015.

[28] J. Andrews *et al.*, "What will 5G be?", *IEEE Journal on Selected Areas in Communications*, vol. 32, no. 6, pp. 1065–1082, 2014.

[29] C. Yang *et al.*, "When ICN meets C-RAN for HetNets: an SDN approach", *IEEE Communications Magazine*, vol. 53, no. 11, pp. 118–125, 2015.

[30] European Telecommunications Standards Institute, *Network functions virtualisation: An introduction, benefits, enablers, challenges & call for action*, Oct. 2012. [Online]. Available: `https://portal.etsi.org/NFV/NFV_White_Paper.pdf`.

[31] D. González G. *et al.*, "A novel multiobjective framework for cell switch-off in dense cellular networks", in *2014 IEEE International Conference on Communications (ICC)*, Jun. 2014, pp. 2641–2647. DOI: `10.1109/ICC.2014.6883722`.

[32] Boingo Wireles Inc.*et al.*, *Office of engineering and technology and wireless telecommunications bureau seek information on current trends in LTE-U and LAA technology, et docket No. 15-105*, Oct. 2015. [Online]. Available: `http://apps.fcc.gov/ecfs/document/view?id=60001330362`.

[33] Wi-Fi Alliance, *Wi-Fi Alliance® statement on License-Assisted Access (LAA)*, Feb. 2015. [Online]. Available: `http://www.wi-fi.org/news-events/newsroom/wi-fi-alliance-statement-on-license-assisted-access-laa`.

[34] 3GPP, "RP-140808: review of regulatory requirements for unlicensed spectrum", Tech. Rep., Jun. 2014.

[35] European Telecommunications Standards Institute, "Broadband radio access networks (BRAN); 5 GHz high performance RLAN; harmonized EN covering the essential requirements of article 3.2 of the R&TTE Directive", Tech. Rep., Jun. 2012. [Online]. Available: http://www.etsi.org/deliver/etsi_en/301800_301899/301893/01.07.01_60/en_301893v010701p.pdf.

[36] S. McGlaun, *4 billion Wi-Fi enabled devices in use around the world today*, Feb. 2014. [Online]. Available: http://www.tweaktown.com/news/35816/4-billion-wi-fi-enabled-devices-in-use-around-the-world-today/index.html.

[37] A. Al-Dulaimi *et al.*, "5G communications race: Pursuit of more capacity triggers LTE in unlicensed band", *IEEE Vehicular Technology Magazine*, vol. 10, no. 1, pp. 43–51, 2015.

[38] LTE-U Forum, *LTE-U technical report, coexistence study for LTE-U SDL V1.0*, Feb. 2015.

[39] ——, *LTE-U CSAT procedure TS V1.0*, Feb. 2015.

[40] ——, *LTE-U SDL coexistence specifications V1.3*, Oct. 2015.

[41] W. Alliance, *Wi-Fi Alliance® aims to harmonizeWi-Fi® and LTE-U coexistence*, Nov. 2015. [Online]. Available: http://www.wi-fi.org/news-events/newsroom/wi-fi-alliance-aims-to-harmonize-wi-fi-and-lte-u-coexistence.

[42] Federal Communications Commission, *The next step for LTE-U: Conducting limited LTE-U performance tests*, Jan. 29, 2016. [Online]. Available: https://www.fcc.gov/news-events/blog/2016/01/29/next-step-lte-u-conducting-limited-lte-u-performance-tests.

[43] Nokia Networks, *The MulteFire opportunity for unlicensed spectrum*, 2015.

[44] F. Abinader *et al.*, "Enabling the coexistence of LTE and Wi-Fi in unlicensed bands", *Communications Magazine, IEEE*, vol. 52, no. 11, pp. 54–61, 2014.

[45] M. Khawer *et al.*, "usICIC–a proactive small cell interference mitigation strategy for improving spectral efficiency of LTE networks in the unlicensed spectrum", *IEEE Transactions on Wireless Communications*, vol. 15, no. 3, pp. 2303–2311, 2016.

[46] H. Song *et al.*, "A spectrum etiquette protocol and interference coordination for LTE in unlicensed bands (LTE-U)", in *2015 IEEE International Conference on Communication Workshop (ICCW)*, IEEE, 2015, pp. 2338–2343.

[47] W. Xu *et al.*, "Lower-complexity power allocation for LTE-U systems: A successive cap-limited waterfilling method", in *2015 IEEE 81st Vehicular Technology Conference (VTC Spring)*, IEEE, 2015, pp. 1–6.

[48] H. Ko *et al.*, "A fair Listen-Before-Talk algorithm for coexistence of LTE-U and WLAN", *IEEE Transaction on Vehicular Technology*, vol. PP, no. 99, 2016.

[49] A. Bhorkar *et al.*, "Performance analysis of LTE and Wi-Fi in unlicensed band using stochastic geometry", in *2014 IEEE 25th Annual International Symposium on Personal, Indoor, and Mobile Radio Communication (PIMRC)*, IEEE, 2014, pp. 1310–1314.

[50] O. Sallent *et al.*, "Learning-based coexistence for LTE operation in unlicensed bands", in *2015 IEEE International Conference on Communication Workshop (ICCW)*, IEEE, 2015, pp. 2307–2313.

[51] A. Voicu *et al.*, "Coexistence of pico-and femto-cellular LTE-unlicensed with legacy indoor Wi-Fi deployments", in *2015 IEEE International Conference on Communication Workshop (ICCW)*, IEEE, 2015, pp. 2294–2300.

[52] F. Chaves *et al.*, "LTE UL power control for the improvement of LTE/Wi-Fi coexistence", in *2013 IEEE 78th Vehicular Technology Conference (VTC Fall)*, IEEE, 2013, pp. 1–6.

[53] A. Sadek *et al.*, "Extending LTE to unlicensed band-merit and coexistence", in *2015 IEEE International Conference on Communication Workshop (ICCW)*, IEEE, 2015, pp. 2344–2349.

[54] C. Cano *et al.*, "Coexistence of WiFi and LTE in unlicensed bands: A proportional fair allocation scheme", in *2015 IEEE International Conference on Communication Workshop (ICCW)*, IEEE, 2015, pp. 2288–2293.

[55] Y. Jian *et al.*, "Coexistence of Wi-Fi and LAA-LTE: Experimental evaluation, analysis and insights", in *2015 IEEE International Conference on Communication Workshop (ICCW)*, IEEE, 2015, pp. 2325–2331.

[56] N. Rupasinghe *et al.*, "Reinforcement learning for licensed-assisted access of LTE in the unlicensed spectrum", in *2015 IEEE Wireless Communications and Networking Conference (WCNC)*, IEEE, 2015, pp. 1279–1284.

[57] X. Mao *et al.*, "Wireless channel modeling methods: Classification, comparison and application", in *2010 5th International Conference on Computer Science & Education*, 2010.

[58] A. Molisch, *Wireless communications*. John Wiley & Sons, 2007.

[59] ITU-R, "M. 2135: Guidelines for evaluation of radio interface technologies for imt-advanced", Tech. Rep., 2009.

[60] P. Almers *et al.*, "Survey of channel and radio propagation models for wireless MIMO systems", *EURASIP Journal on Wireless Communications and Networking*, vol. 2007, no. 1, pp. 1–19, 2007.

[61] Y. Sawaragi *et al.*, *Theory of Multiobjective Optimization*, 1st. Academic Press, Inc., 1985.

[62] C. Coello *et al.*, *Evolutionary Algorithms for Solving Multi-Objective Problems*, 2nd. Springer: Genetic and Evolutionary Computation Series, 2007.

[63] A. Konak *et al.*, "Multi-objective optimization using genetic algorithms: A tutorial", *Reliability Engineering & System Safety*, vol. 91, no. 9, pp. 992–1007, 2006.

[64] M. Pilát, "Evolutionary multiobjective optimization: A short survey of the state-of-the-art", *Proceedings of the Contributed Papers Part I-Mathematics and Computer Sciences, WDS, Prague, Czech*, pp. 1–4, 2010.

[65] Z. Zhou *et al.*, "Multiobjective evolutionary algorithms: A survey of the state of the art", *Swarm and Evolutionary Computation*, vol. 1, no. 1, pp. 32–49, 2011.

[66] K. Deb *et al.*, "A fast and elitist multiobjective genetic algorithm: NSGA-II", *IEEE Transactions on Evolutionary Computation*, vol. 6, no. 2, pp. 182–197, Apr. 2002.

[67] S. Caban *et al.*, *Evaluation of HSDPA and LTE: From testbed measurements to system level performance*. John Wiley & Sons, 2011.

[68] M. Sacristán *et al.*, "LTE-Advanced system level simulation platform for IMT-Advanced evaluation", Waves, 2011.

[69] European Telecommunications Standards Institute, "TS 136 213; LTE;evolved universal terrestrial radio (E-UTRA);physical layer procedures", 2011.

[70] U. Paul *et al*, "Understanding traffic dynamics in cellular data networks", in *2011 IEEE International Conference on Computer Communications (INFOCOM)*, Apr. 2011, pp. 882–890.

[71] D. Lee *et al.*, "Spatial modeling of the traffic density in cellular networks", *Wireless Communications, IEEE*, vol. 21, no. 1, pp. 80–88, 2014.

[72] D. González G. *et al.*, "Topology and irregularity in cellular networks", in *Wireless Communications and Networking Conference (WCNC), 2015 IEEE*, IEEE, 2015, pp. 1719–1724.

[73] A. Papoulis *et al.*, *Probability, random variables, and stochastic processes*. Tata McGraw-Hill Education, 2002.

[74] AWE Communications, *ProMan (integrated in Atoll) user reference*, 2003. [Online]. Available: `http://www.awe-communications.com/Docs/ProMan_UrbanDLLReference.pdf`.

[75] Group Radio Access Network, *TR 25.892: feasibility study for orthogonal frequency division multiplexing (OFDM) for UTRAN enhancement*, v6.0.0, 3GPP, Jun. 2004.

[76] F. Lima *et al.*, "Scheduling for improving system capacity in multiservice 3GPP LTE", *Journal of Electrical and Computer Engineering*, vol. 2010, p. 3, 2010.

[77] R. Jain *et al.*, "Throughput fairness index: An explanation", Tech. rep., Department of CIS, The Ohio State University, Tech. Rep., 1999.